AD-A111 404 ARMY MISSILE COMMAND REDSTONE ARSENAL AL ADVANCED S--ETC F/G 17/9
FREQUENCY DIVERSE TARGET SCINTILLATION FOR TARGET CLASSIFICATIO--ETC(U)
FEB 81 P M ALEXANDER, M C SCHEXNAYDER

UNCLASSIFIED ORSMI-RE-81-11-TR SBI-AD-E950 204 NL

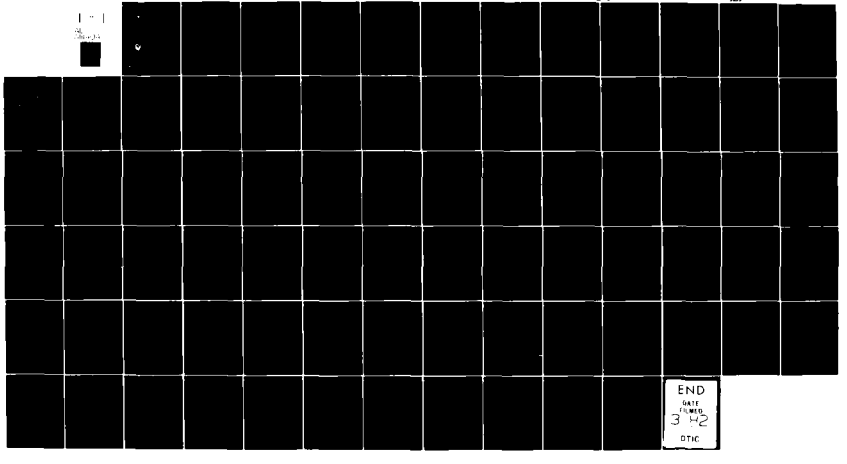

END
DATE FILMED
3-82
DTIC

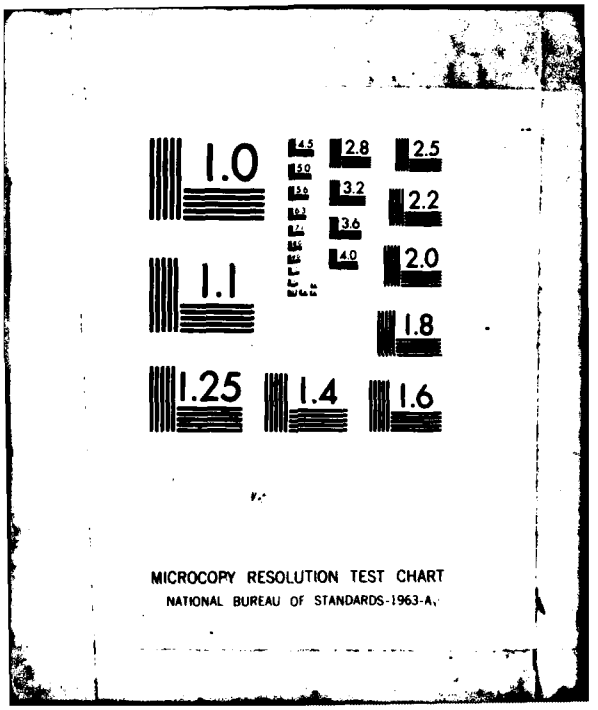
1.0
1.1
1.25
1.4
1.6
1.8
2.0
2.2
2.5
2.8
3.2
3.6
4.0
MICROCOPY RESOLUTION TEST CHART
NATIONAL BUREAU OF STANDARDS-1963-A

TECHNICAL REPORT RE-81-11

FREQUENCY DIVERSE TARGET SCINTILLATION FOR TARGET CLASSIFICATION USING MILLIMETER WAVE RADAR

Dr. P. Martin Alexander
CPT Michael C. Schexnayder
Advanced Sensors Directorate
US Army Missile Laboratory

18 February 1981

U.S. ARMY MISSILE COMMAND
Redstone Arsenal, Alabama 35898

DISPOSITION INSTRUCTIONS

DESTROY THIS REPORT WHEN IT IS NO LONGER NEEDED. DO NOT RETURN IT TO THE ORIGINATOR.

DISCLAIMER

THE FINDINGS IN THIS REPORT ARE NOT TO BE CONSTRUED AS AN OFFICIAL DEPARTMENT OF THE ARMY POSITION UNLESS SO DESIGNATED BY OTHER AUTHORIZED DOCUMENTS.

TRADE NAMES

USE OF TRADE NAMES OR MANUFACTURERS IN THIS REPORT DOES NOT CONSTITUTE AN OFFICIAL INDORSEMENT OR APPROVAL OF THE USE OF SUCH COMMERCIAL HARDWARE OR SOFTWARE.

UNCLASSIFIED

SECURITY CLASSIFICATION OF THIS PAGE (When Data Entered)

REPORT DOCUMENTATION PAGE

READ INSTRUCTIONS BEFORE COMPLETING FORM

1. REPORT NUMBER: TR-RE-81-11	2. GOVT ACCESSION NO.: AD-A111 404
3. RECIPIENT'S CATALOG NUMBER:	
4. TITLE (and Subtitle): Frequency Diverse Target Scintillation for Target Classification Using Millimeter Wave Radar	5. TYPE OF REPORT & PERIOD COVERED: Technical Report
	6. PERFORMING ORG. REPORT NUMBER:
7. AUTHOR(s): Dr. P. Martin Alexander CPT Michael C. Schexnayder	8. CONTRACT OR GRANT NUMBER(s):
9. PERFORMING ORGANIZATION NAME AND ADDRESS: Commander, US Army Missile Command ATTN: DRSMI-REL Redstone Arsenal, AL 35898	10. PROGRAM ELEMENT, PROJECT, TASK AREA & WORK UNIT NUMBERS:
11. CONTROLLING OFFICE NAME AND ADDRESS: Commander, US Army Missile Command ATTN: DRSMI-RE Redstone Arsenal, AL 35898	12. REPORT DATE: 18 February 1981 13. NUMBER OF PAGES: 78
14. MONITORING AGENCY NAME & ADDRESS(if different from Controlling Office):	15. SECURITY CLASS. (of this report): UNCLASSIFIED 15a. DECLASSIFICATION/DOWNGRADING SCHEDULE:

16. DISTRIBUTION STATEMENT (of this Report)

Approved for public release; distribution unlimited.

17. DISTRIBUTION STATEMENT (of the abstract entered in Block 20, if different from Report)

18. SUPPLEMENTARY NOTES

19. KEY WORDS (Continue on reverse side if necessary and identify by block number)

Millimeter Waves	Continuous Wave Radar
Frequency Diversity	Fourier Transforms
Target Classification	Computer Simulation
Scintillations	

20. ABSTRACT (Continue on reverse side if necessary and identify by block number)

The phenomenon of target radar cross section dependence on transmitted frequency was investigated as a candidate technique for target classification. Over a frequency diverse bandwidth, the received signal amplitude will scintillate, and these scintillations can be analyzed to determine target characteristics. An experimental 94 GHz radar system was designed, built, and used to obtain experimental results for corner reflector targets. Theoretical computer simulations were developed and compared to the experimental data, and

DD FORM 1 JAN 73 1473 EDITION OF 1 NOV 65 IS OBSOLETE

UNCLASSIFIED

SECURITY CLASSIFICATION OF THIS PAGE (When Data Entered)

20 (con't)

agreement was quite good, considering the radar system limitations. Some of the data was Fourier analyzed and compared with theoretical spectra. It was concluded that the reflex klystron used is not adequate to obtain data from complex targets. Suggestions for further research are given.

CONTENTS

A

ILLUSTRATIONS

ILLUSTRATIONS (concluded)

TABLES

I. INTRODUCTION

In the work described in this report, the phenomenon of target radar cross section dependence on transmitted frequency was investigated as a candidate technique for target classification. Very simply, the phenomenon results from the fact that a target consists of several individual reflectors which constructively or destructively interfere, depending on their range separation and on the tranmitted frequency. Thus, over a given frequency diverse bandwidth, the received signal amplitude will fluctuate or scintillate, and these scintillations can be analyzed to determine target characteristics.

Frequency diversity has long been investigated as a method of improving target detection[1-4], tracking accuracy [5-7], and range resolution.[8] More recently, frequency diverse target scintillation has been studied as a technique for acquisition and classification of stationary targets.[9-13] Also, frequency diversity, combined with polarization diversity, has been investigated both experimentally and theoretically; in these techniques, amplitudes and relative phases are measured to obtain stationary target signatures.[14-18]

The purpose of the present experimental effort was to design and build a 94 GHz radar and to evaluate the utility of the radar for detecting frequency diverse radar cross section effects. A few additional measurements were made with a 140 GHz radar, and these data are also presented and discussed.

In Section II, a brief theoretical analysis of expected results is outlined. Descriptions of the two radar systems used in this experiment are given in Section III, and the signal processing and measurement techniques are also discussed.

Experimental data taken for corner reflectors at various range spacings are presented in Section IV. The frequency calibration method used is described, and range separation values obtained with radar results are compared with measured values.

For the 94 GHz data, a computer simulation program was developed for comparison. A description of the program is given in Section V, while, in Section VI, the agreement and discrepancies between the theoretical and experimental results are discussed.

Finally, in Section VII, conclusions from the simulated and experimental results are drawn with respect to radar characteristics, and recommendations for further research are given.

II. MATHEMATICAL ANALYSIS

Consider a target consisting of n reflectors with radar cross sections (RCS) σ_1, σ_2, σ_3, . . . σ_n. Assume that the target is stationary and that all reflectors are equally illuminated by the radar. The target is in the far-field of the radar, and vice versa. Assume also that the typical linear dimension of the reflectors is much larger than the transmitted wavelength (optical region). In general, the RCS of the individual reflectors will vary as the frequency squared, as for flat plates and corner reflectors. However,

the frequency diverse bandwidth is assumed to be sufficiently small that these changes in RCS are negligible.

Let R_{ij} be the range to the ith reflector, and define

$$R_i = \left| R_j - R_i \right| , \tag{1}$$

that is, R_{ij} is the range separation between the ith and the jth reflector. It can be shown that, for a continuous wave radar, the square-law detected signal voltage, V(f), is given by[13]

$$\begin{aligned} V(f) = A \{ & \sigma_1 + \sigma_2 + \sigma_3 + \ldots\ldots + \sigma_n \\ & + 2\sqrt{\sigma_1\sigma_2} \cos\left[2\pi \left(\frac{2R_{12}}{c}\right) f\right] \\ & + 2\sqrt{\sigma_1\sigma_3} \cos\left[2\pi \left(\frac{2R_{13}}{c}\right) f\right] \\ & + 2\sqrt{\sigma_2\sigma_3} \cos\left[2\pi \left(\frac{2R_{23}}{c}\right) f\right] \\ & + \ldots \} \end{aligned} \tag{2}$$

or

$$V(f) = A \left\{ \sum_{i=1}^{n} \sigma_i + \sum_{\substack{i=1 \\ i\neq j}}^{n} \sum_{j=1}^{n} \sqrt{\sigma_i\sigma_j} \cos\left[2\pi \left(\frac{2R_{ij}}{c}\right) f\right] \right\}. \tag{3}$$

Here A is a parameter depending on target range, transmitted power, and characteristics of the radar; c is the speed of light, and f is the transmitted frequency.

If the voltage signal is measured as a function of frequency, there is a constant "dc" level and a superposed "ac" waveform which is periodic with frequency.

The result is analogous to a time domain periodic wave form; here time is analogous to frequency, and frequency is analogous to the quantitiy

$$f_{ij} = \frac{2R_{ij}}{c} . \tag{4}$$

Note that this "frequency" f_{ij} is the time it takes electromagnetic energy to make a round trip between the ith and jth reflectors.

Equation (3) shows that, mathematically, the Fourier transform of V(f) is already performed. The transform of V(f) should show a spike of amplitude

$$A_{ij} = 2A\sqrt{\sigma_i \sigma_j} \tag{5}$$

at a "frequency" of f_{ij} (Equation (4)).

Each pair of reflectors contributes a spike to the Fourier transform, although two pairs with equal range separation contribute to the same spike and, thus, cannot be distinguished. However, a high degree of structural periodicy in the target, i.e., many reflectors with equal spacing, would result in a strong spike at the characteristic range separation. The number of contributions to the Fourier transform spectrum increases in an arithmetic series with the number of reflectors; for n reflectors, there are $\frac{1}{2}n(n-1)$ contributing pairs.

All the experimental data taken were for two or three reflectors. For the two reflector case, the V(f) (or "interference pattern") is given by

$$V(f) = A\left\{\sigma_1 + \sigma_2 + 2\sqrt{\sigma_1 \sigma_2}\cos\left[2\pi\left(\frac{2R_{12}}{c}\right) f\right]\right\} \tag{6}$$

i.e., a single sinusoidal oscillation. For three reflectors,

$$\begin{aligned} V(f) = A\{&\sigma_1 + \sigma_2 + \sigma_3 \\ &+ 2\sqrt{\sigma_1 \sigma_2}\cos\left[2\pi\left(\frac{2R_{12}}{c}\right) f\right] \\ &+ 2\sqrt{\sigma_1 \sigma_3}\cos\left[2\pi\left(\frac{2R_{13}}{c}\right) f\right] \\ &+ 2\sqrt{\sigma_2 \sigma_3}\cos\left[2\pi\left(\frac{2R_{23}}{c}\right) f\right]\} \end{aligned} \tag{7}$$

so that V(f) in this case is a superposition of three sinusoidal oscillations.

In terms of these oscillations, one complete cycle will be observed when the cosine argument changes by 2π, or when the change in frequency, Δf, is such that

$$\Delta f = \frac{c}{2R_{ij}}. \tag{8}$$

The frequency diverse bandwidth (Δf) required to see one complete oscillation in V(f) is calculated in Table 1 for various reflector separations. The values were chosen to aid in understanding the experimental data.

TABLE 1. FREQUENCY DIVERSE BANDWIDTHS.

Reflector Range Separation R_{ij} (Meters)	Frequency Diverse Bandwidth Required for One Cycle in V(f) (MHz)
10	15.0
6	25.0
5	30.0
4	37.5
3	50
2	75
1	150
0.5 (50 cm)	300
0.1 (10 cm)	1.5 GHz
0.01 (1 cm)	15 GHz

III. DESCRIPTION OF RADAR SYSTEMS

A. 94 GHz Radar System

The 94 Ghz radar system is depicted in Figure 1. The millimeter source is a continuous wave (cw) klystron with a nominal power of 300 mW and a nominal electronic tuning 3 dB bandidth of 200 MHz. The klystron reflector voltage is sawtooth wave modulated at a 1 KHz repetition rate to sweep the klystron over its entire tuning range. Some of the output is coupled to a thermistor for monitoring the power. Also, some of the power is coupled through a cavity wavemeter (for ballpark frequency measurements) to a square law detector (for monitoring the transmitted power waveform). The power at the transmit antenna for this experiment is estimated to be about 200 mW. A linear vertically polarized wave was transmitted.

The receiver consists of an antenna, a square law detector with a sensitivity of about 600 mV/mW, and a low noise preamplifier used at a gain of ten and an input impedance of 1 MegOhm. The receive signals were monitored with a low bandwidth (500 KHz) high sensitivity (100μV/division) oscilloscope triggered by a 1 KHz sync pulse from the waveform generator. As shown in Figure 1, the received waveform consisted of the broad "interference pattern" (received signal vs klystron reflector voltage) during the sawtooth rise, and a compressed version during the sawtooth fall.

This signal was applied to a boxcar averager/gated integrator, also triggered at 1 KHz by the waveform generator. The boxcar averager provides a variable size aperature which may be positioned anywhere during the received interference pattern. The gated integrator is operated in the exponential averaging mode, which provides a weighted average output; that is, the most recent pulses have more influence than early pulses. The output of the boxcar averager can be considered to be the average of 2 TC/AD repetitions of the signal falling within the aperture, where TC is the selected integration time constant and AD is the selected aperture duration. For this experiment, TC=1.0 s and AD~10 s, so there was essentially no pulse integration.

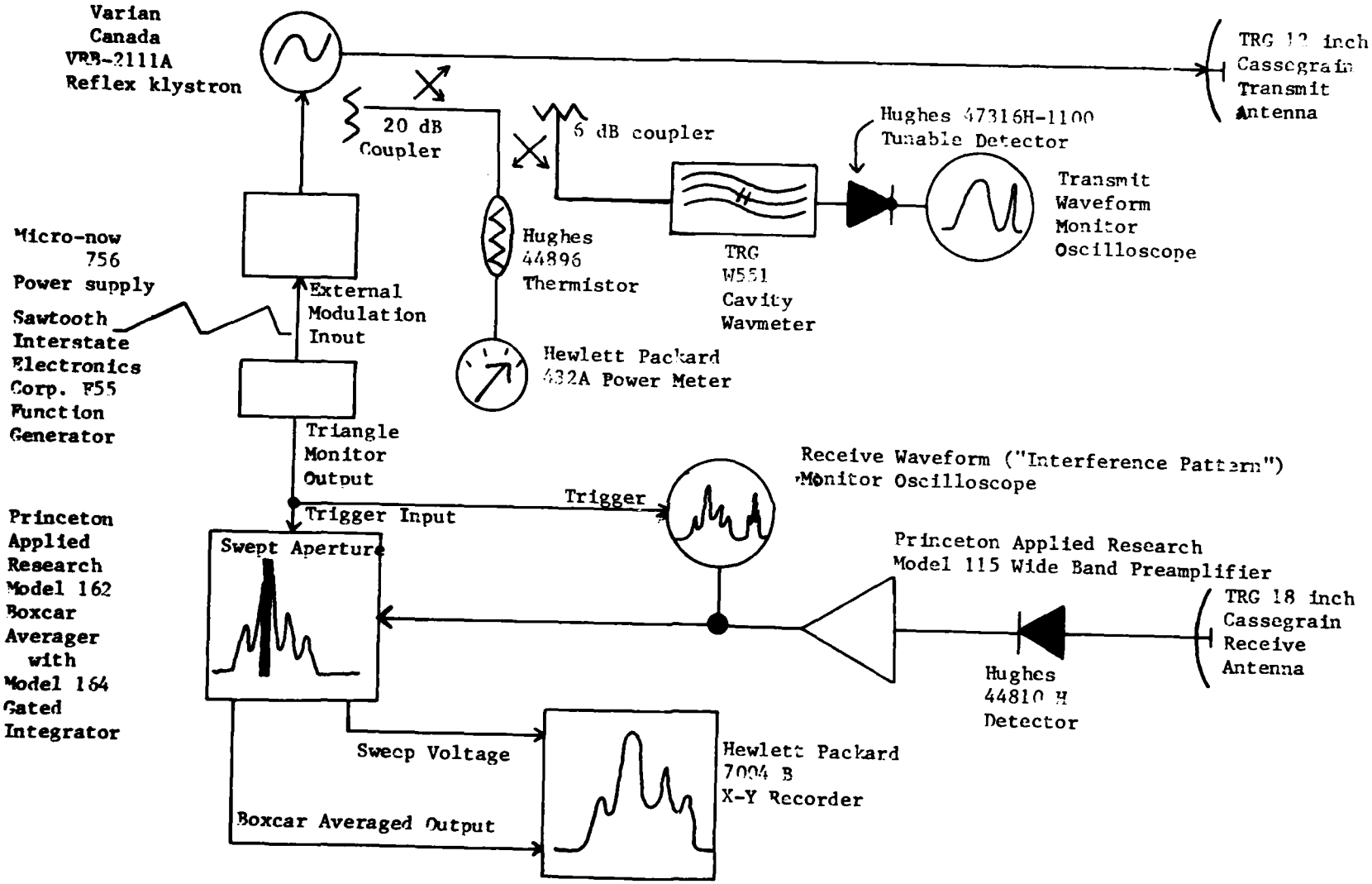

Figure 1. Millimeter radar system.

The boxcar averager provides for the automatic scan of the aperture between selected limits and also provides a scan voltage proportional to the aperture position. Thus, data were taken by sweeping the aperature once across the broad interference pattern and plotting boxcar integrator output vs scan voltage (or, equivalently, reflector voltage) on an X-Y recorder. The sweep time was about 18 s, and a boxcar integrator signal time constant of 0.1 s (low pass filter) provided some smoothing of the interference pattern.

B. 140 GHz Radar System

The characteristics of the 140 GHz radar have been documented extensively and specifications are presented in Tables 2-4.[19] The frequency of the radar is manually adjustable over a 600 MHz bandwidth. Data were taken by measuring the pulse height of the target response on an oscilloscope (A-scope) as a function of frequency. Only the observed maxima and minima points were recorded.

TABLE 2. TRANSMITTER PERFORMANCE SPECIFICATIONS.

TRANSMITTER - Coherent/Pulse Compression	
Operating Frequency	142.02 GHz
Transmitted Peak Power	10 mW (10 dBm)
Equivalent Peak Power	600 mW (28 dBm)
Transmitted Pulse Width	3 usec
Compressed Pulse Width	50 nsec
Chirp Bandwidth	20 MHz
Pulse Compression Ratio	60
PRF	30 kHz
Pulse Repetition Interval	33.3 usec
Duty Cycle	9%
Average Transmitted Power	0.9 mW
Frequency Diversity Bandwidth	660 MHz

TABLE 3. RECEIVER PERFORMANCE SPECIFICATIONS.

RECEIVER - Pulse-Doppler with Pulse Compression	
First LO Frequency	140.67 GHz
First IF Frequency	1395 MHz
Second LO Frequency	1275 MHz
Second IF Frequency	120 MHz
Noise Figure (SSB) of First Mixer	13 dB
First Mixer Preamplifier Gain	26 dB minimum
Circulator Frequency Range	142 + 1 GHz
Circulator Isolation	18 dB minimum
Circulator Insertion Loss	1.6 dB maximum
Circulator VSWR	1.40 maximum
Unambiguous Range	~5 km
Receiver Bandwidth	24 MHz
SAW Line Bandwidth	25 MHz
Range Cell (3-usec pulse)	1500 ft
Range Cell (50-nsec pulse)	25 ft

TABLE 4. TRACKING/GUIDANCE ANTENNA SPECIFICATIONS.

Type	Cassegrain, Conscan
Operating Frequency	142 GHz
Diameter (ℓ)	60 cm
3-dB Beamwidth ($\theta_B \sim \lambda/\ell$)	0.23° = 4.0 mrad (0.23° = 4.0 mrad)
Gain ($G_D \sim 4\pi A/\lambda 2$)	56.2 dB (59 dB) (→ efficiency ~ 50%)
Sidelobe Level	-16.3 dB
Crossover Points	3 dB ↔ 2.0 mrad offset 1.5 dB ↔ 1.1 mrad offset
VSWR	1.15
Polarization	Linear, Vertical
Conical Scan Rate	30 to 90 Hz
Angle of First Sidelobe	(~ 6 mrad)
Far Field ($R > 2D^2/\lambda$)	(R > 340 m)

IV. EXPERIMENTAL RESULTS

A. 94 GHz Radar Data

The measurements made with the 94 GHz radar were taken in the High Bay area of Building 5400, Redstone Arsenal, Alabama. The target range was ~80 meters, satisfying far-field conditions for both radar and target. The transmit and receive antennas were side-by-side, and their centers were approximately 1 meter above the concrete floor. Antenna beamwidths are 0.4° and 0.6°, so that the antenna main lobes did not intersect the floor at the target (no main lobe multipath). The 3 dB beamwidths of the transmit and receive antennas overlapped each other by approximately 30 cm at the target.

The first data taken were a series for the two corner reflectors separated by 6, 5, 4, 3, 2, and 1 meters. These results are shown in Figures 2-7. The corner reflectors were triangular trihedrals with RCS of 200 sm and 91 sm. The larger corner reflector was behind and above the smaller corner reflector. The scales shown on the data are relative amplitudes (uncalibrated); the klystron reflector voltage range is about 100 V, while the video output (boxcar integrator output) is on the order of millivolts. These data show the expected result--a single oscillation modified by the transmitter power curve. As a measure of the transmitter (and receiver) power curve, data were taken for the transmit waveform monitor output (Figure 8) and for each corner reflector separately (Figure 9 and 10). The power curve of Figure 8 is similar to typical reflex klystron power output characteristics (Figure 11).[20] Using the boxcar aperature in conjunction with the cavity wavemeter, the total operating range was determined to be approximately from 93.96 Ghz to 94.11 Ghz (± 0.01 GHz), or a total of about 150 MHz. The center frequency (maximum power point) was 94.05 GHz. The 3 dB electronic tuning bandwidth is around 100 MHz, which is about half that claimed by the manufacturer.

The klystron frequency is clearly not a linear function of reflector voltage, so the data obtained for 2 reflectors separated by 6 meters was used to calibrate frequency change vs reflector voltage change. These calibration

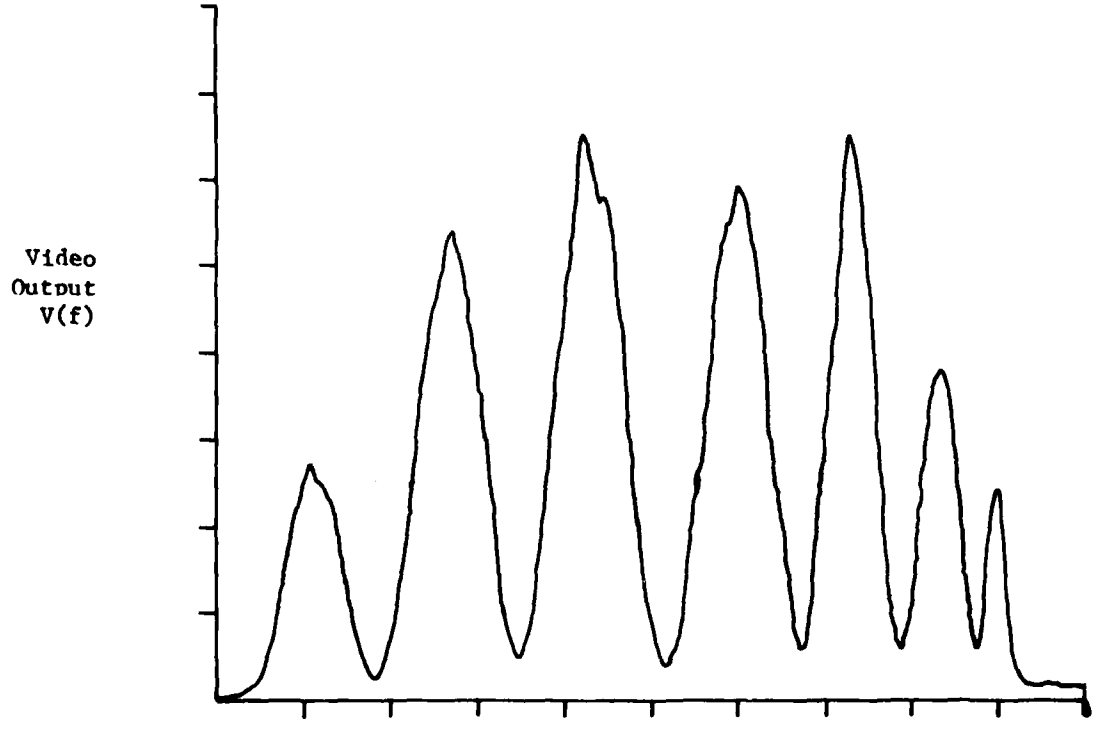

Figure 2. Two reflectors separated by 6 meters.

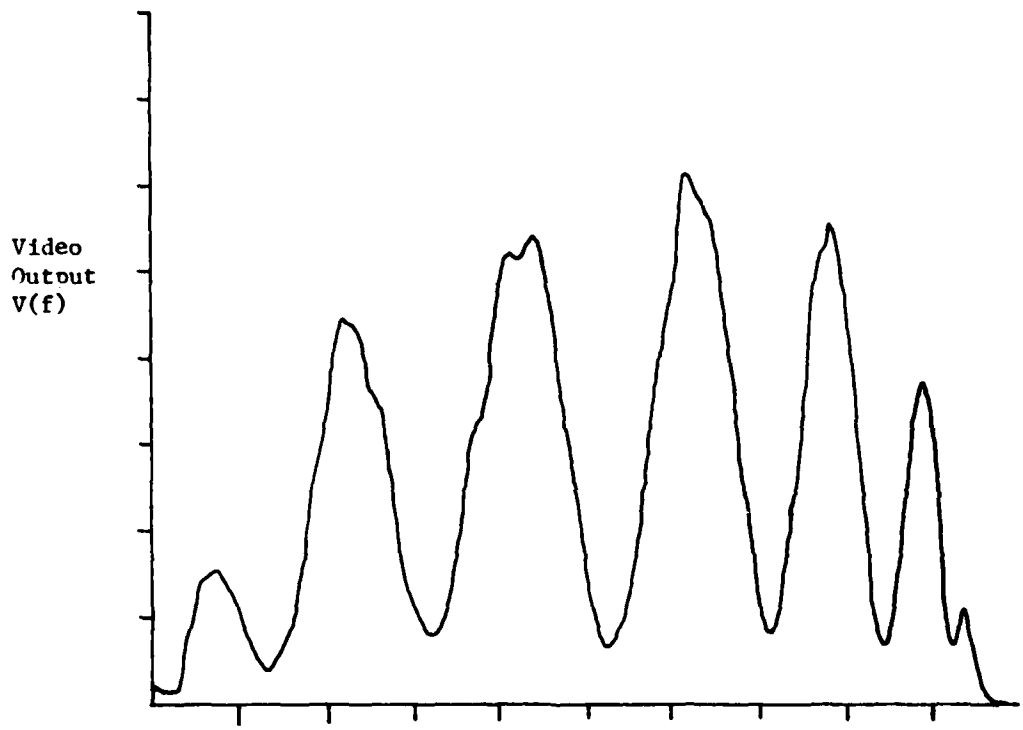

Figure 3. Two reflectors separated by 5 meters.

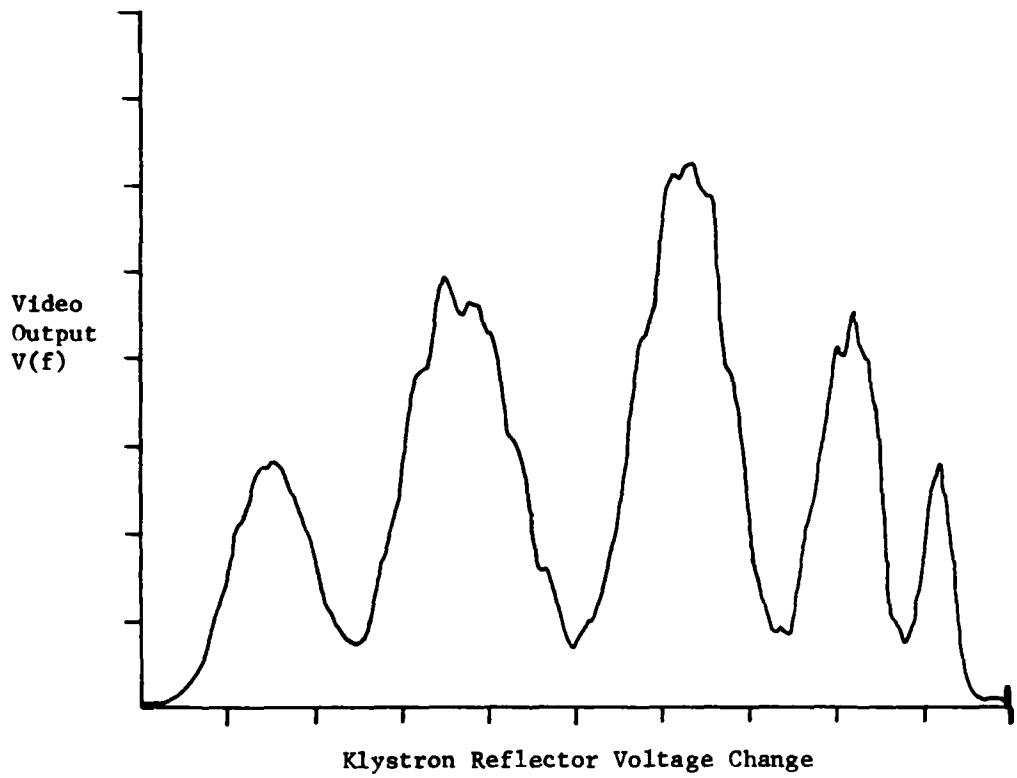

Figure 4. Two reflectors separated by 4 meters.

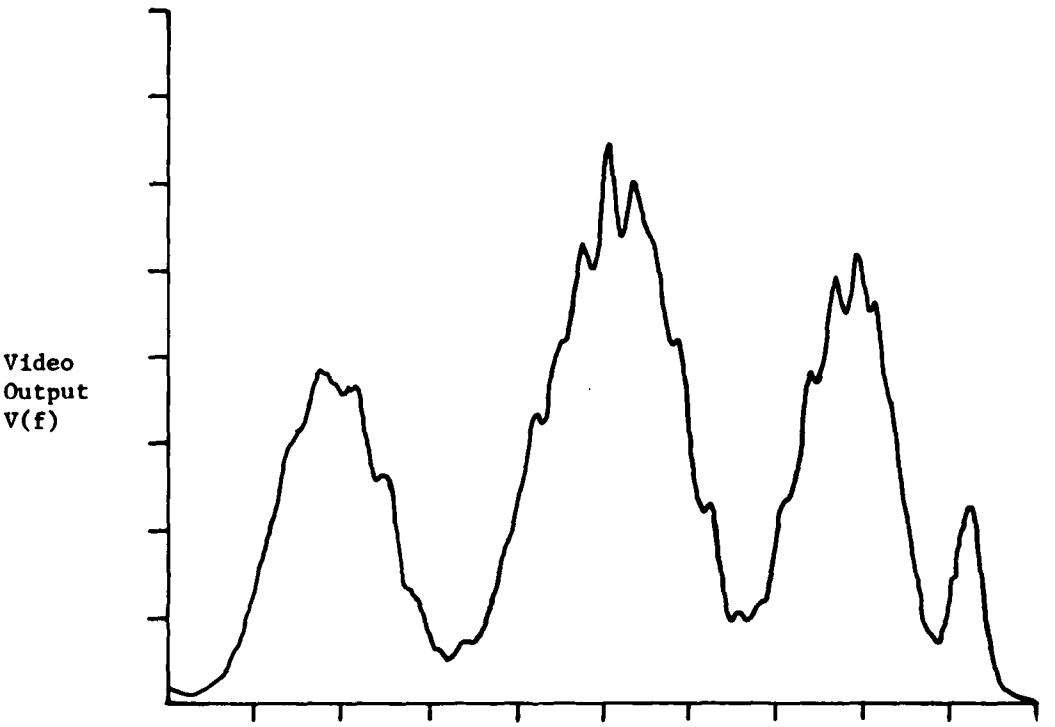

Figure 5. Two reflectors separated by 3 meters.

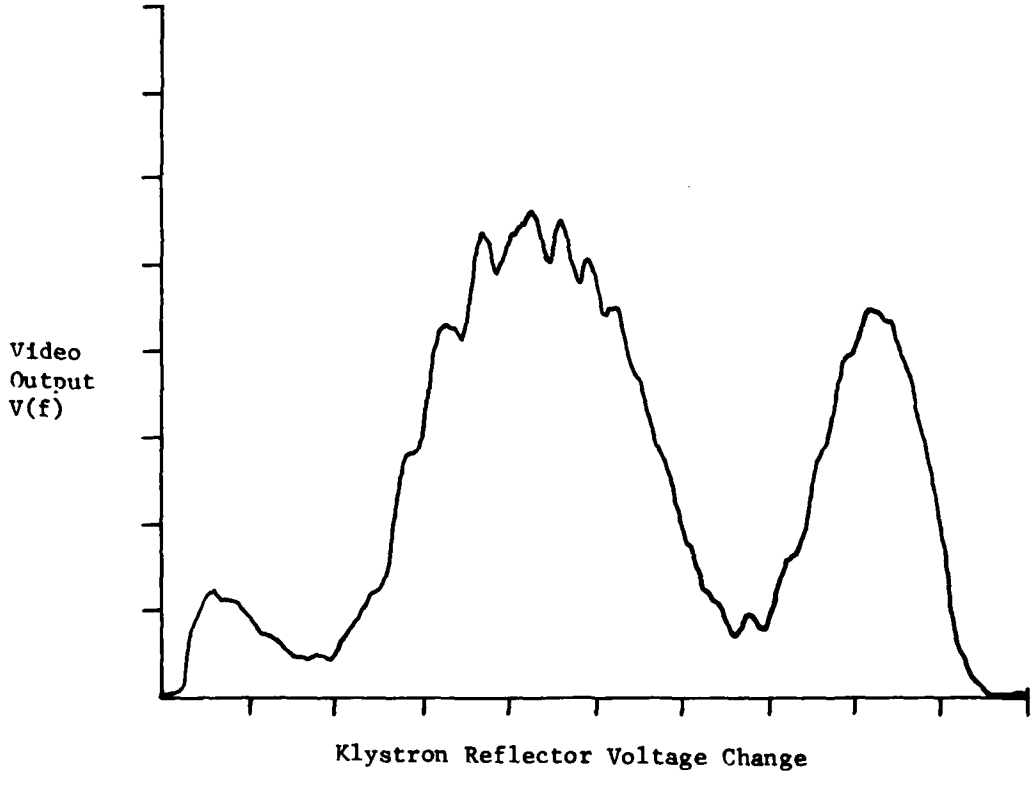

Figure 6. Two reflectors separated by 2 meters.

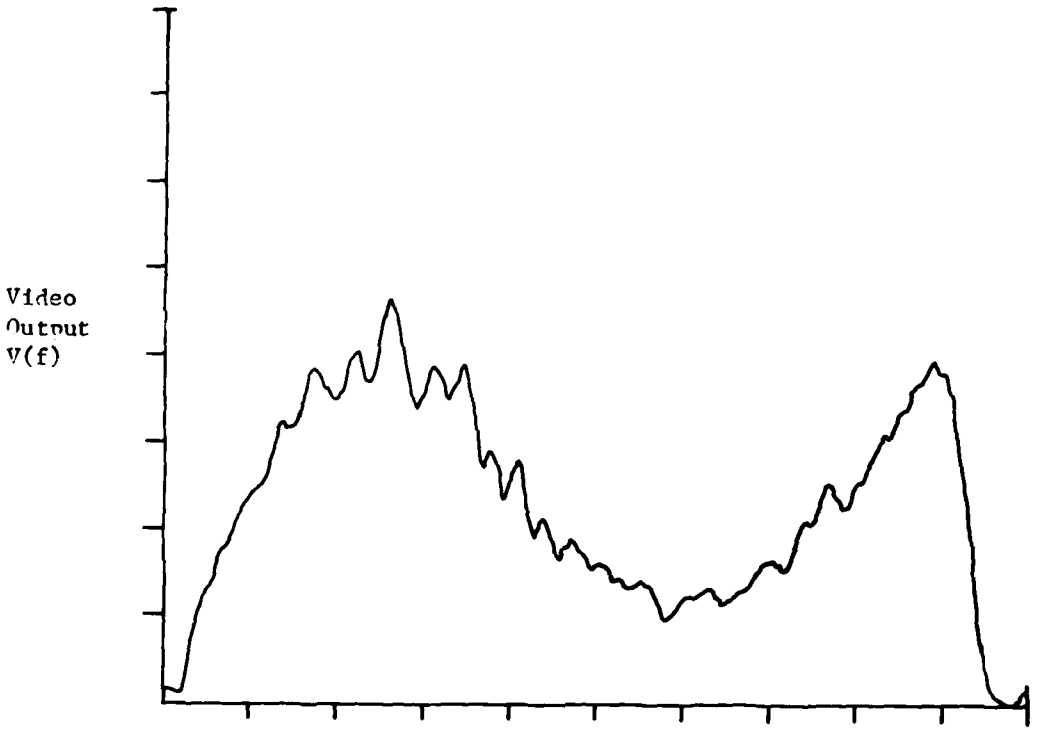

Figure 7. Two reflectors separated by 1 meter.

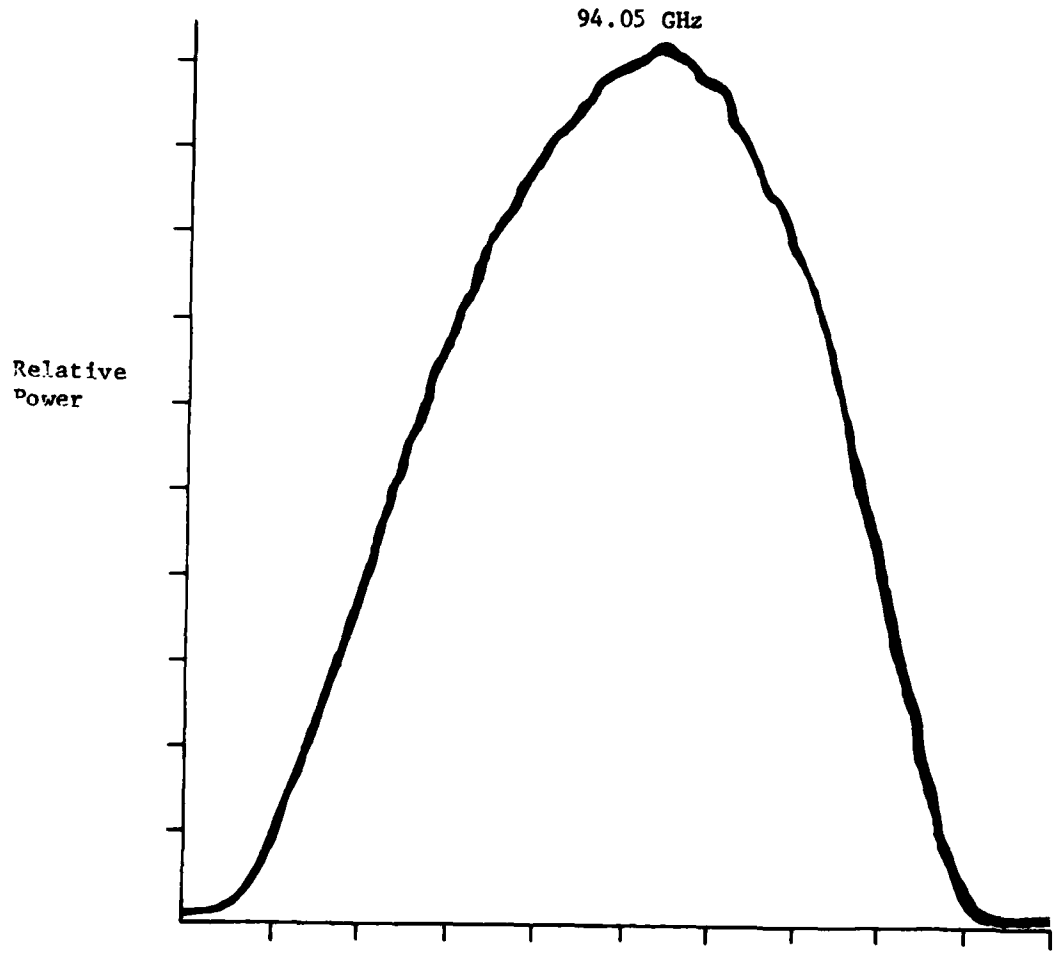

Figure 8. Transmitter power curve.

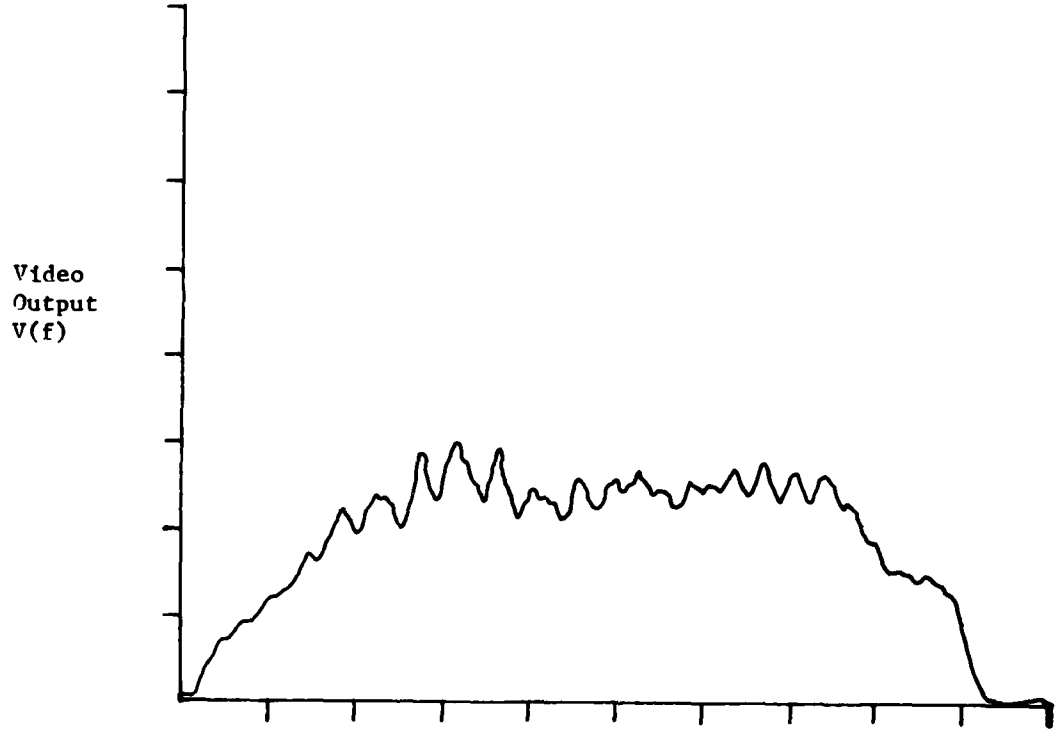

Figure 9. 200 sm reflector only.

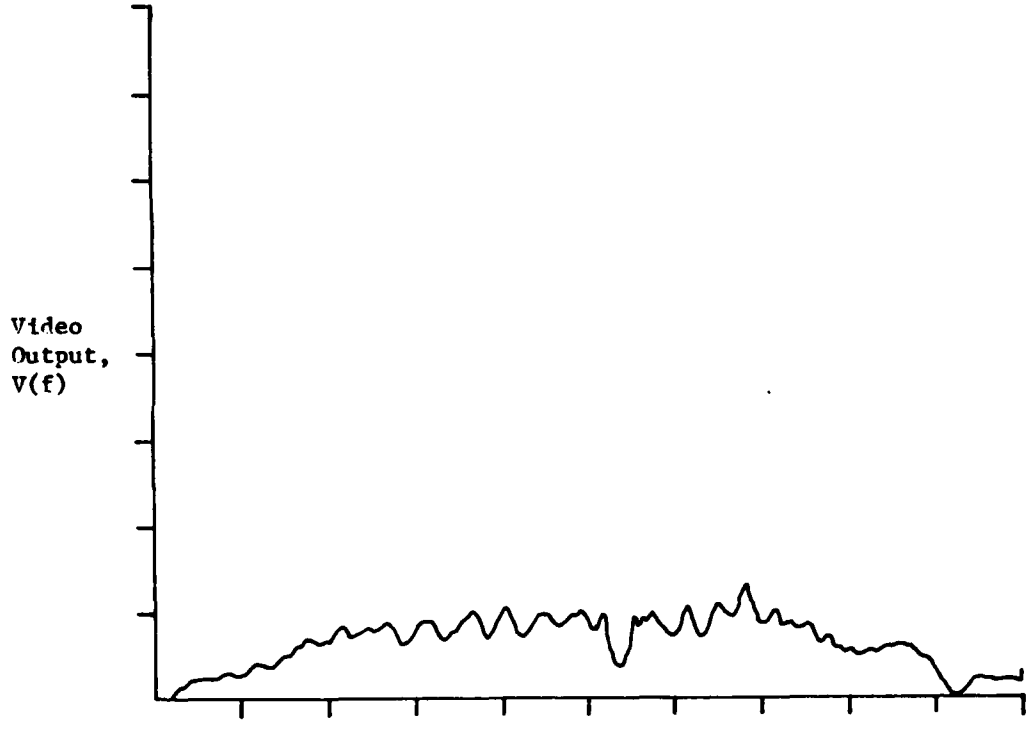

Klystron Reflector Voltage Change

Figure 10. 91 sm reflector only.

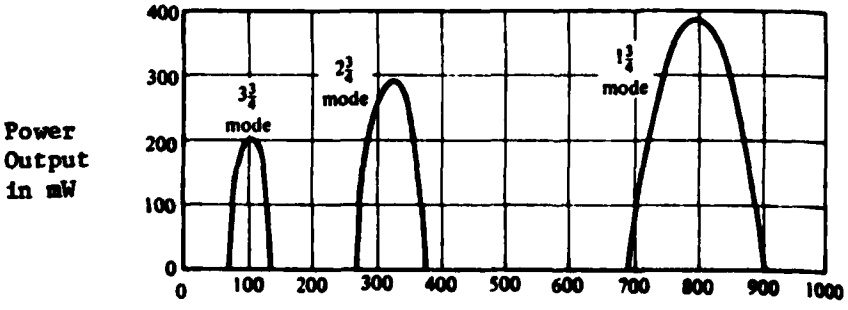

Klystron Reflector Voltage in Volts

Figure 11. Power output characteristics of a reflex klystron (after Liao).

data were then used to analyze the results for other separations and, in particular, compare the range separation calculated from the radar data to the actual range separation as determined with a tape measure.

Figure 12 indicates how the calibration was made. The position of each maxima and minima, indicated by a vertical line, was estimated to the nearest one half linear unit by bisecting the given half cycle at its half height. These data are given in Table 5. From Table 1, it is seen that, for a 6 meter separation, the maxima are 25 MHz apart, so that the extrema are 12.5 MHz apart. The first maximum was arbitrarily assigned a value of 25 MHz. The data of Table 5 are plotted in Figure 13; typical frequency characteristics shown in Figure 14 are similar.[20]

TABLE 5. FREQUENCY CHANGE CALIBRATION DATA

Extrema	Klystron Reflector Voltage Change (linear units)	Change In Frequency (MHz)
Maximum #1	11.0	25.0*
Minimum #1	18.0	37.5
Maximum #2	27.0	50.0
Minimum #2	34.5	62.5
Maximum #3	42.5	75.0
Minimum #3	51.5	87.5
Maximum #4	60.0	100.0
Minimum #4	67.0	112.5
Maximum #5	72.5	125.0
Minimum #5	79.0	137.5
Maximum #6	83.0	150.0
Minimum #6	87.5	162.5

*Arbitrarily Assigned

For the data in Figures 3-7, the number of cycles observed and the reflector voltage change for these cycles were determined. The corresponding frequency change was then found from Figure 13, and the distance between reflectors was calculated from Equation (8) in the form

$$\left(\frac{2\Delta R}{c}\right)\Delta f = (\#\text{ of cycles}) \tag{9}$$

or

$$\Delta R = \frac{c(\#\text{ of cycles})}{2\Delta F} \tag{10}$$

where Δf is now the frequency change over the number of cycles observed. The results of the radar data are compared with the actual separations in Table 6. The actual separations were determined with a tape measure between the front edges of the corner reflectors. Because the phase centers of the reflectors

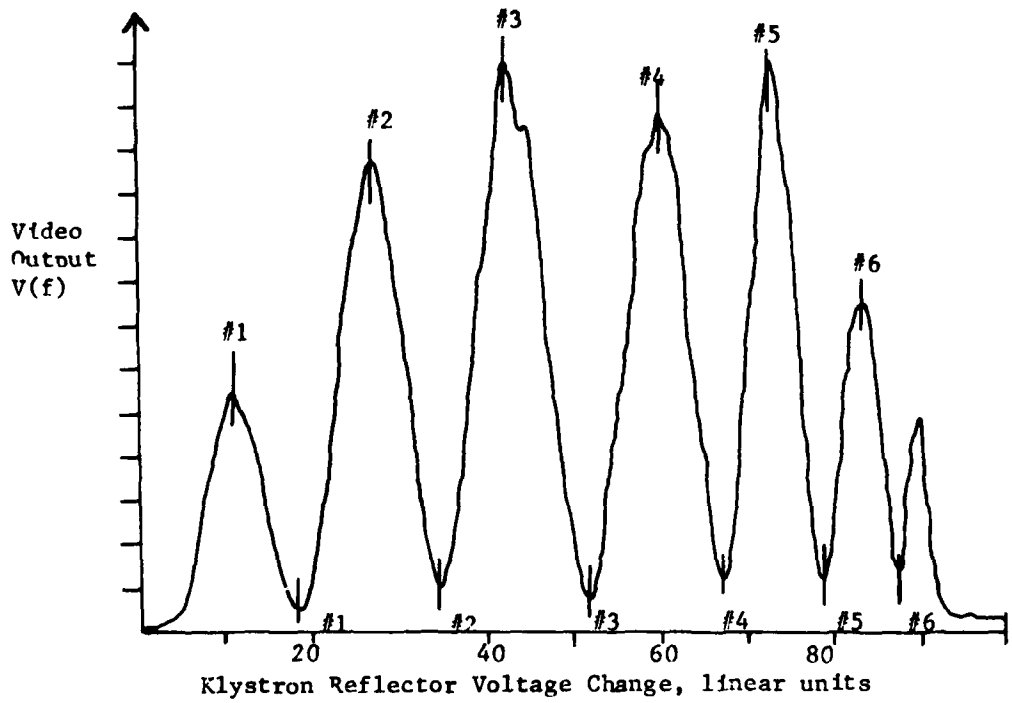

Figure 12. Two reflectors separated by 6 meters: maxima and minima locations.

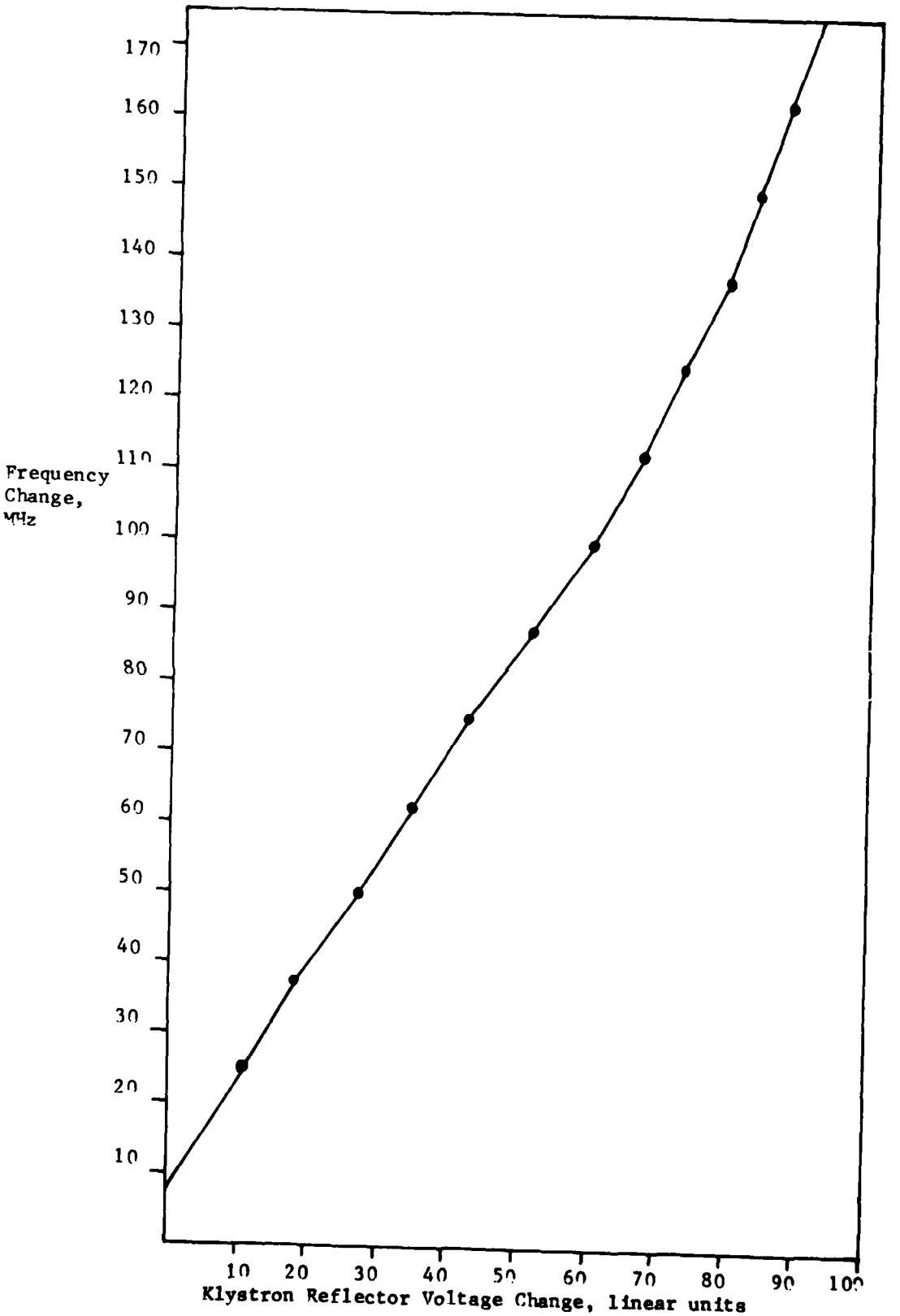
Frequency Change, MHz
170
160
150
140
130
120
110
100
90
80
70
60
50
40
30
20
10
10 20 30 40 50 60 70 80 90 100
Klystron Reflector Voltage Change, linear units

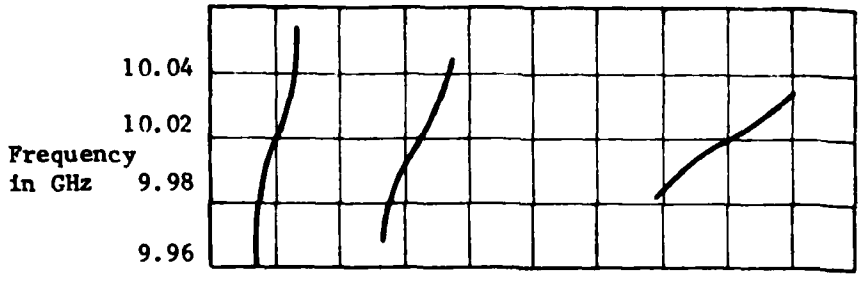

Figure 14. Frequency characteristics of a reflex klystron (after Liao).

are not precisely known, the estimated error for this measurement is ± 10 cm. The agreement is quite good, better than the estimated error, except for the one meter separation case, where the power curve severely distorts the interference pattern.

TABLE 6. REFLECTOR SEPARATION DETERMINED FROM RADAR DATA

Measured Separation	Number of Cycles Observed	Frequency Change (MHz)	Calculated Separation (meters)	Percent Error
5.0	4½	136	4.96	0.8%
4.0	3½	132	3.98	0.5%
3.0	2½	125.5	2.99	0.3%
2.0	1½	110.5	2.04	2.0%
1.0	½	51	1.47	47.0

An explanation of the fine structure (small oscillations) in some of the data, particularly Figures 5, 6, 7, 9, and 10, is required. The large (~30 ft by 35 ft), flexible metal door of the High Bay was approximately 20 meters behind the corner reflectors. The radar boresight was at an oblique angle to the door, so that under normal conditions no energy was reflected from the door back to the radar. However, when the door was buffeted by the wind, bringing it more perpendicular to boresight, its effect could clearly be seen in the radar signal. The period of the oscillations is consistent with the distance between the door and target.

Two interference patterns were recorded for a target consisting of three corner reflectors. A 50 sm reflector was placed between the two initially used. For the first pattern (Figure 15), the spacing was 4 meters between the first and second and 2 meters between the second and third; for the second pattern (Figure 16), the spacing was 3 meters and 2 meters. These patterns, clearly more complex than those for two reflectors, are analyzed and compared with simulated data in Section 6.

B. 140 GHz Radar Data

The measurements made with the 140 GHz radar were taken at the Road Test Course Area, Redstone Arsenal, Alabama. The target range was about 480 meters, and two triangular trihedral corner reflectors of approximately 5,000 sm and 6,000 sm were used. Only the extrema were measured on an oscilloscope while manually changing the transmitted frequency. The frequency calibration method is described elsewhere.[19]

The interference patterns for two different reflector separations are shown in Figure 17 and Figure 18. Calculations of the radar range separation of the corner reflectors using the radar data gave 1.61 meters and 2.85 meters; both values agree with the measued values within about 5%. Clearly, the data suffer from nonlinearities in the receiver or transmitter. This effect is further demonstrated in the response for a single corner reflector (Figure 19), taken at a range of 400 meters. It is expected that such extreme nonlinearities will make analysis of results for more than two reflectors essentially impossible.

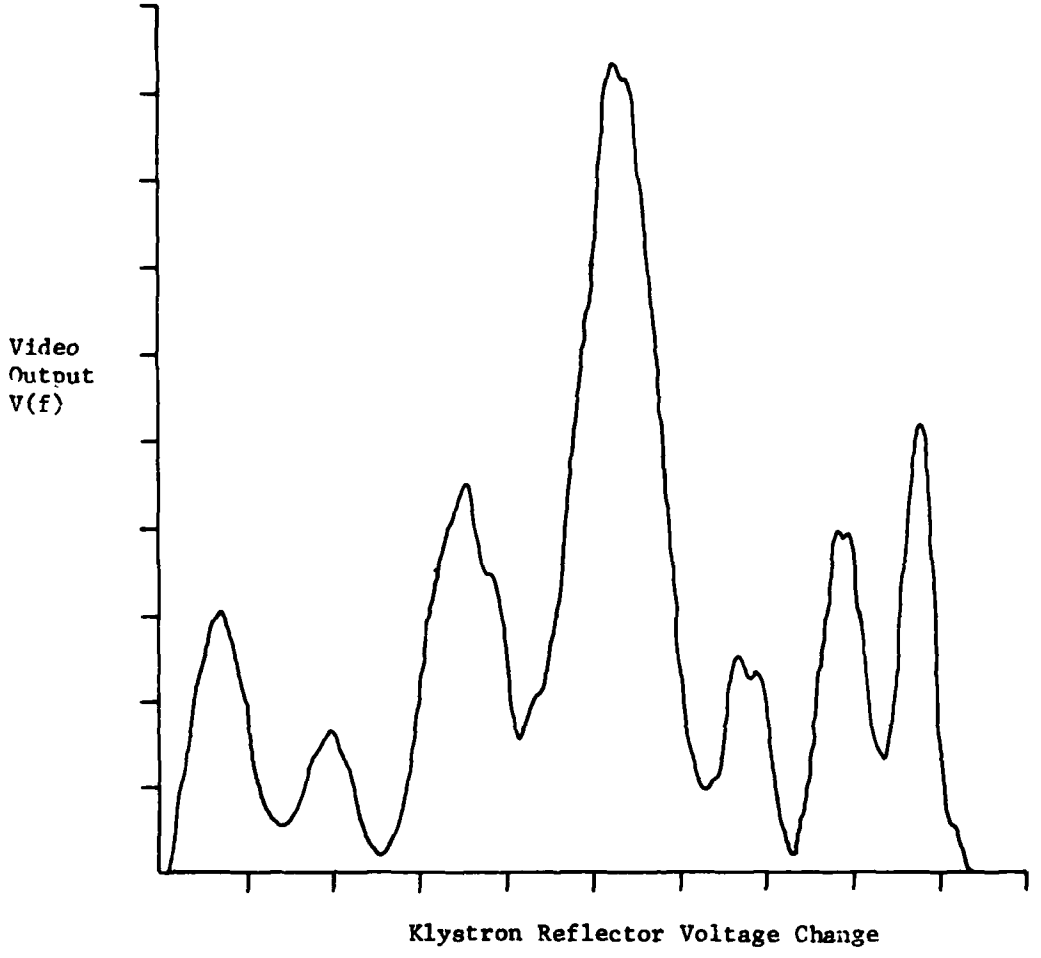

Figure 15. Three reflectors separated by 4m, 2m.

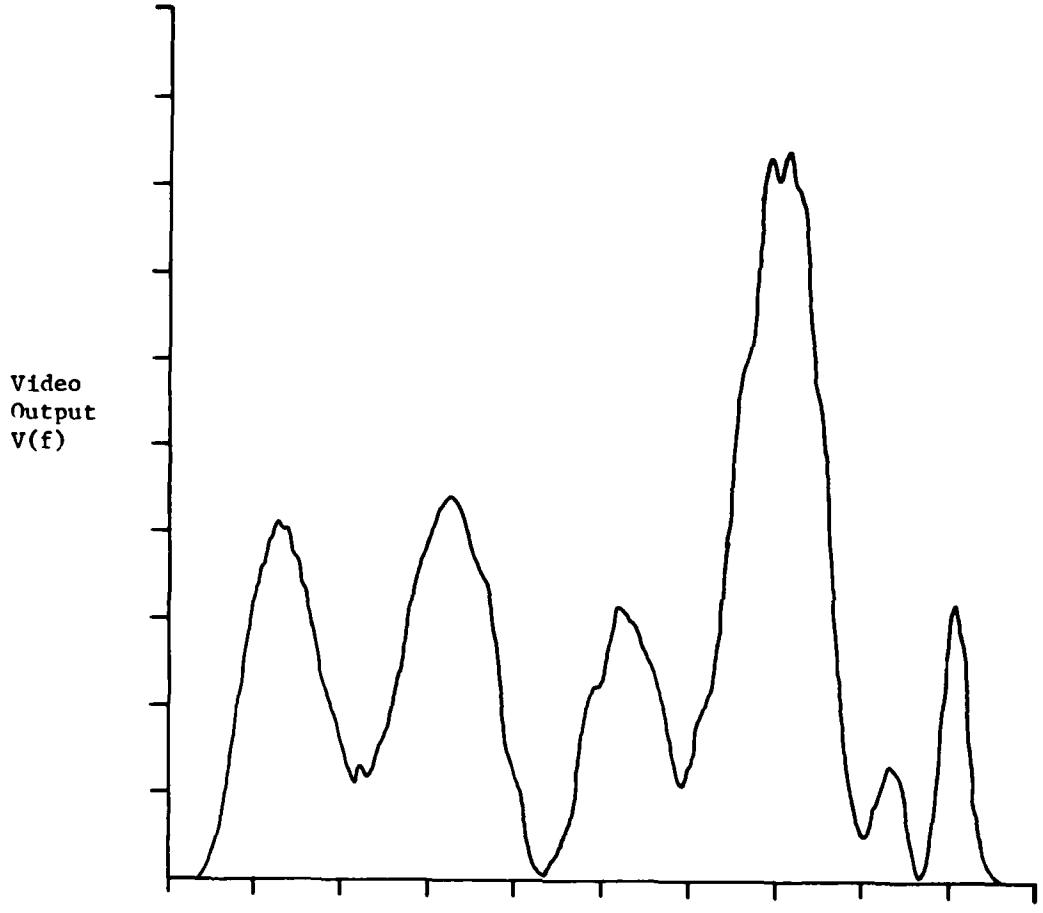

Figure 16. Three reflectors separated by 3m, 2m.

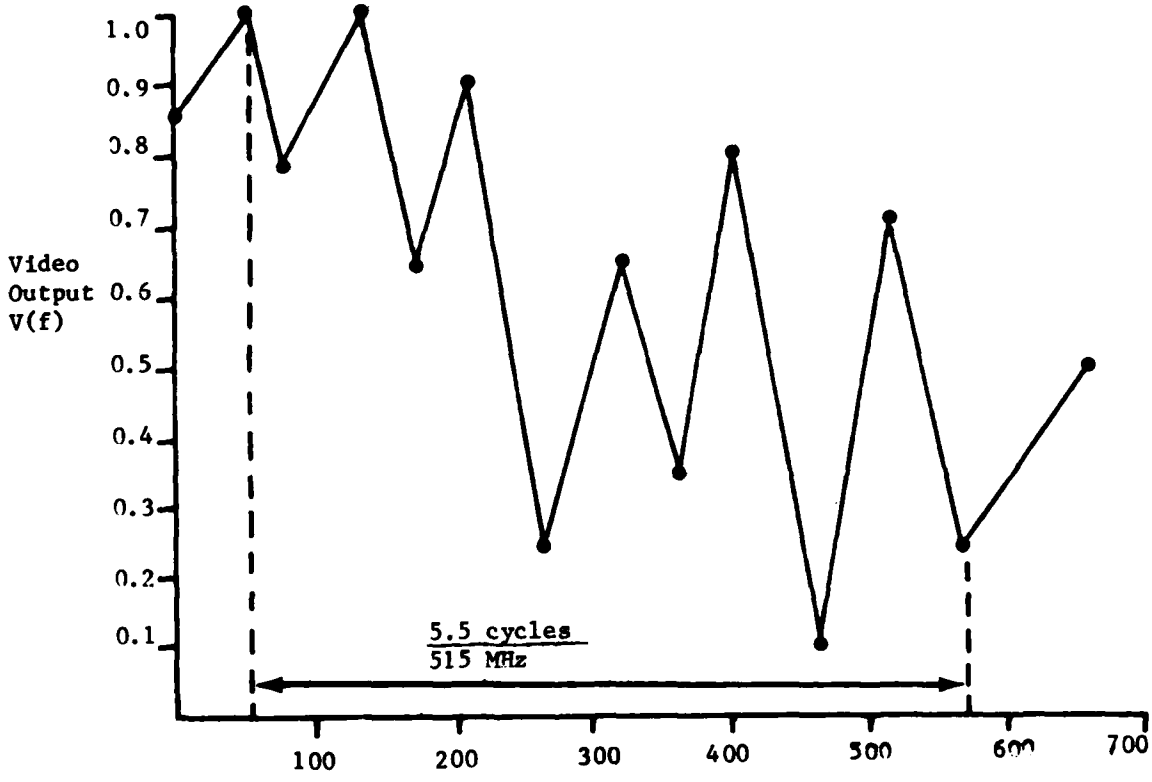

Figure 17. Two reflectors separated by 1.7 meters.

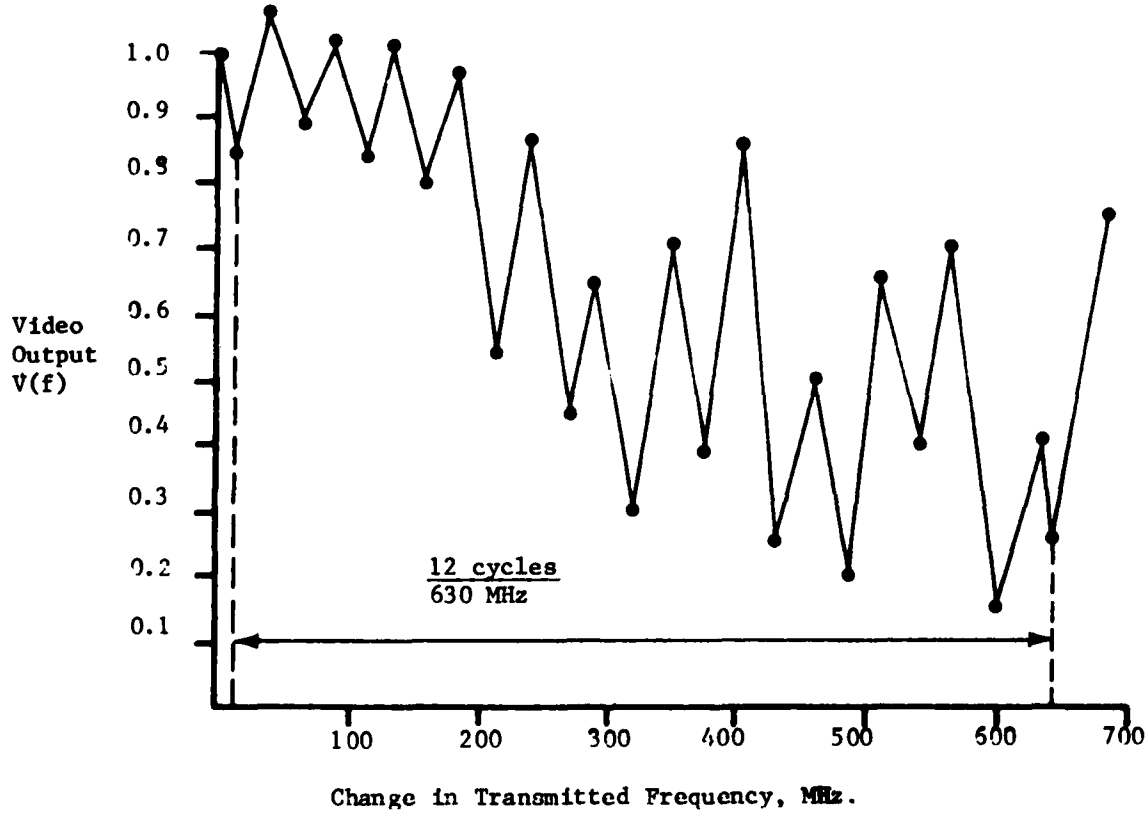

Figure 18. Two reflectors separated by 3.0 meters.

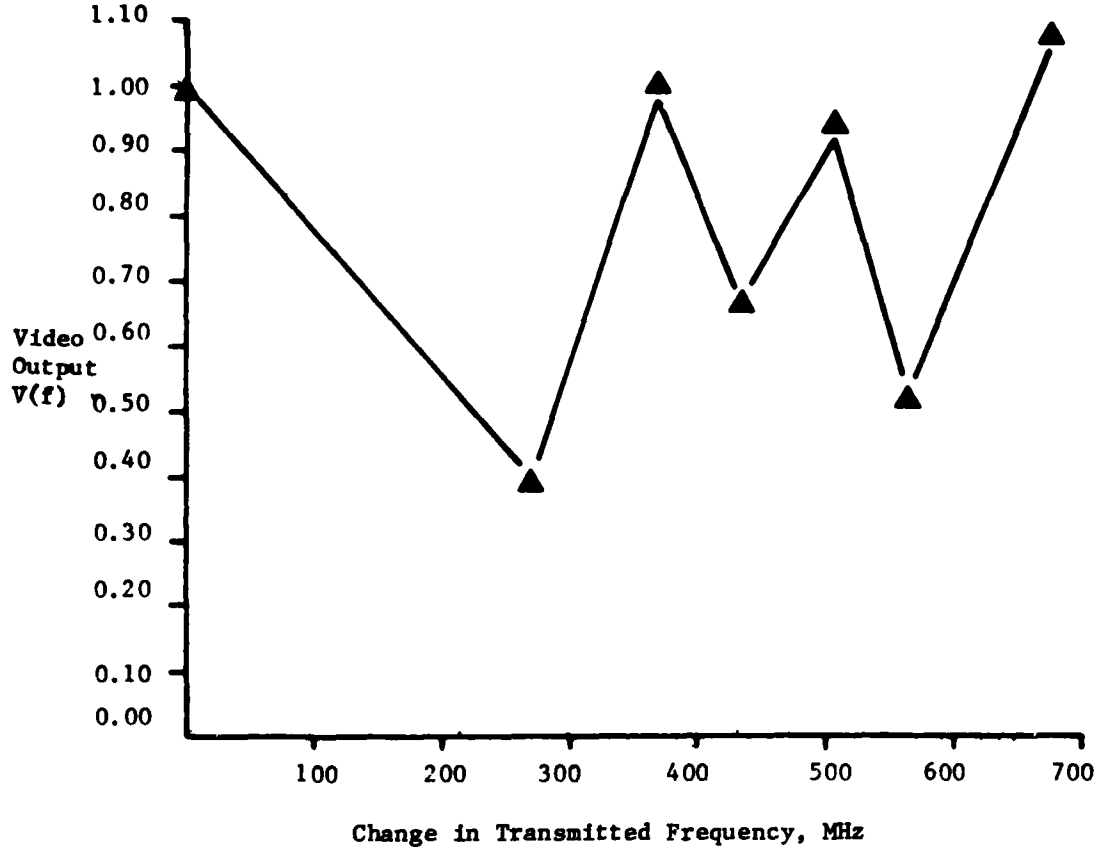

Figure 19. Single corner reflector response.

V. COMPUTER SIMULATION

A computer simulation was developed to compare theoretical versus measured results. Figure 20 details the sequence of actions in the program which develops the theoretical response of the square law detector as the voltage of the source is swept. Since the frequency output of the source is not linear with the applied slewing (reflector) voltage, the plots are amplitude versus slewing voltage. Figure 21 provides the sequence of actions resulting in the discrete Fourier transform (DFT) of the theoretical result. The FFT algorithm used to compute the DFT has been modified to compute the DFT on a computer (HP #9830) which does not have a COMPLEX statement. The modification divides all operations and coefficients into real and imaginary parts.

The HP #9830 uses a type of BASIC (peculiar to HP machines). The actual programs are shown in Appendices A and B. A simple way of inputing the N square law responses is to use the LINK command in the appropriate spot in the square law detector response program (after statement number 620). This is necessary for a small machine such as the HP #9830, since the programs are on cassette tape and no statement equivalent to the FORTRAN CALL statement exists in the HP BASIC language used. The program in Appendix C has the LINK command, directing the program to the FFT routine stored as program 2 on the cassette tape. In order to use this feature, the number of frequency steps must be a power of 2. The maximum number of steps allowed by the structuring of the machine is 256.

VI. COMPARISON OF EXPERIMENTAL AND THEORETICAL RESULTS

For the case of two reflectors, Figures 22 through 29 show a comparison of simulation (dashed curves) and experimental results (solid curves). The simulation results shown include weighting by the power spectrum shown in Figure 8 and the nonlinear frequency dependence on reflector voltage. The frequency of modulation produced by the simulation is nearly identical to the measured data. The relative amplitudes of the peaks in the experimental data fall between the results obtained with the ideal (flat) power spectrum and those obtaiined by weighting the simulation with the power spectrum of Figure 8.

Figure 30 demonstrates the effect of temperature on the output frequency of the klystron oscillator. The specification sheet indicates that the Varian VRB-2111A reflex klystron has a typical frequency/temperature coefficient of -1.6 MHz/^{o}C; all of the simulation results used this value. The effect of this coefficient is to introduce a constant phase shift into the interference patterns. This mechanism was used to adjust the phase of the simulated results to agree with the experimental results, and the temperature correction factors are shown in the figures.

The phase of the signal is really of no importance, since the desired information is the Fourier transform of the measured data. Other sources of slow frequency instability, such as power supply voltages will contribute a phase factor which may be considered to be constant for a given measurement.

The effect of the nonlinear frequency dependence is to cause a changing periodicity in the interference patterns. Figure 13 shows that the slope becomes steeper on the frequency versus voltage curve at the upper end,

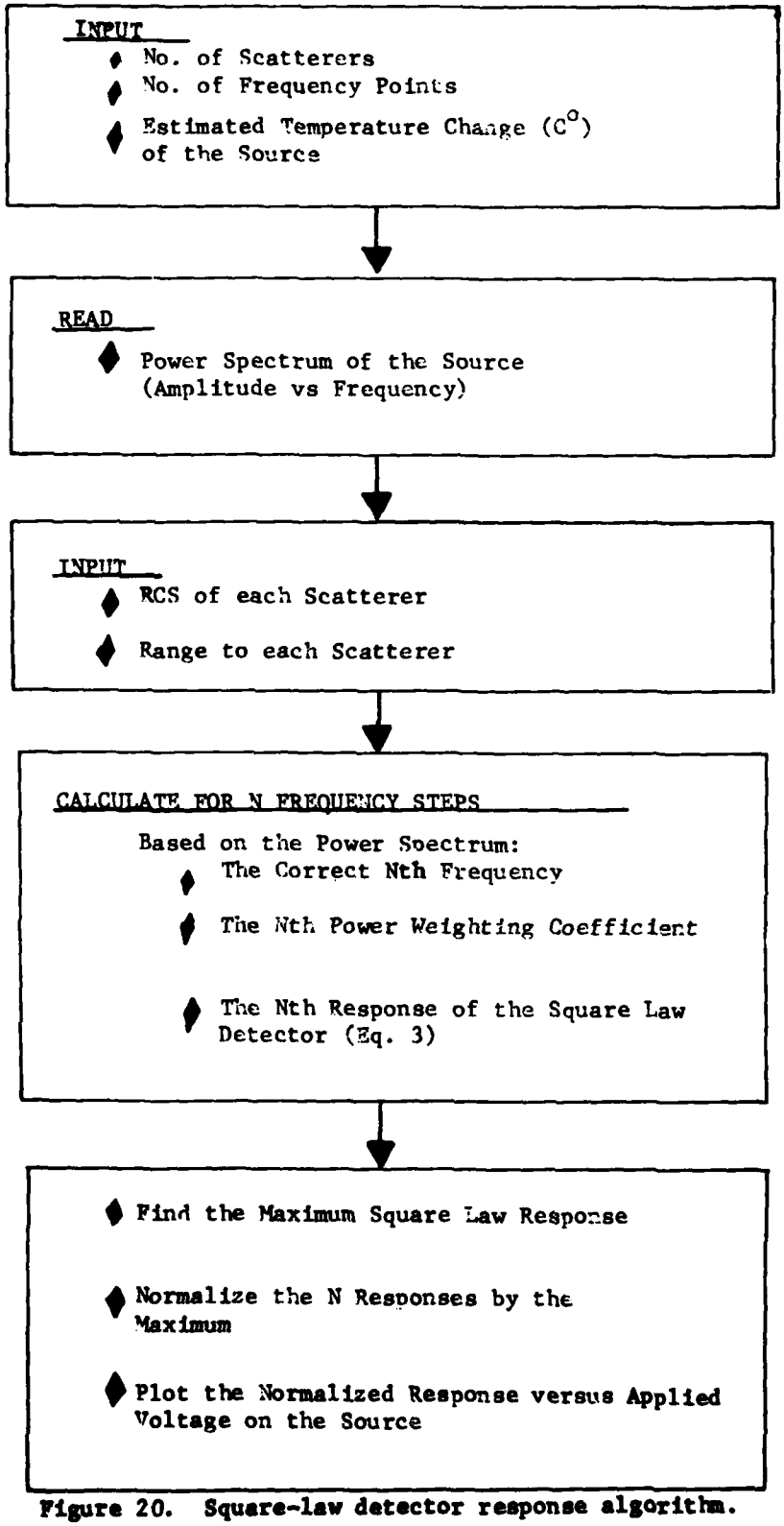

Figure 20. Square-law detector response algorithm.

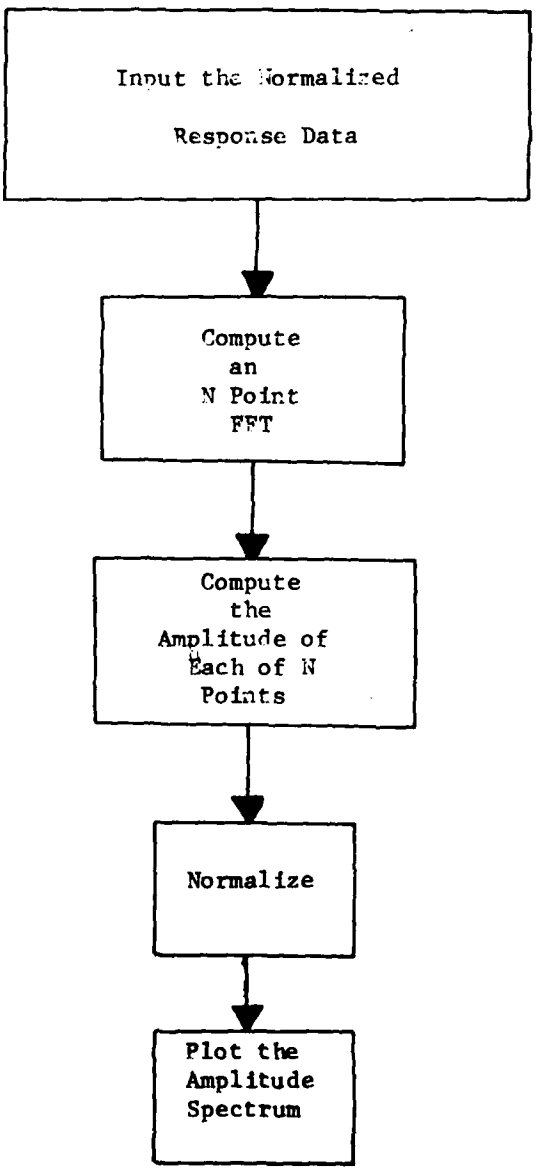

Figure 21. Discrete Fourier transform algorithm.

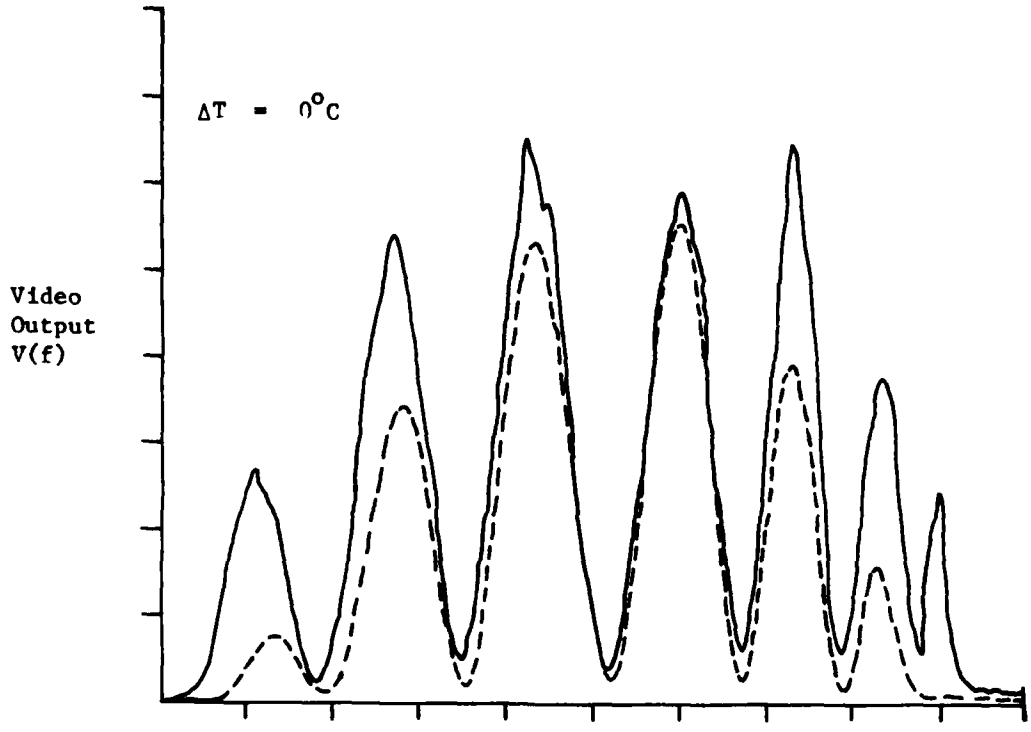

Figure 22 Simulation: two reflectors separated by 6 meters.

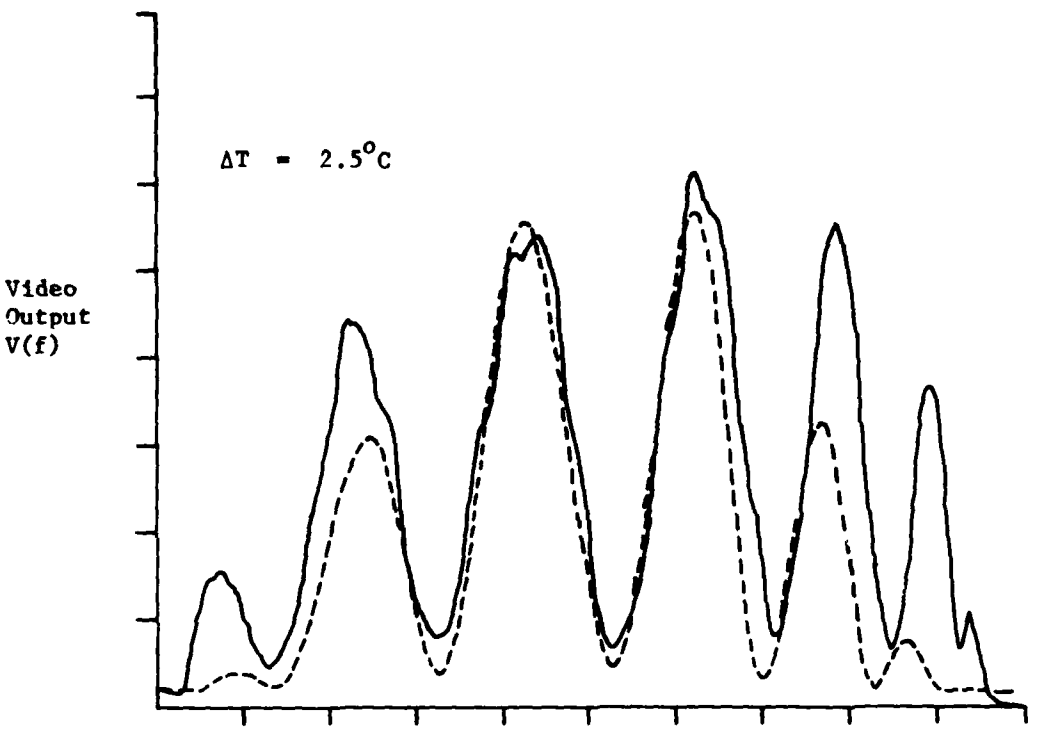

Figure 23. Simulation: two reflectors separated by 5 meters.

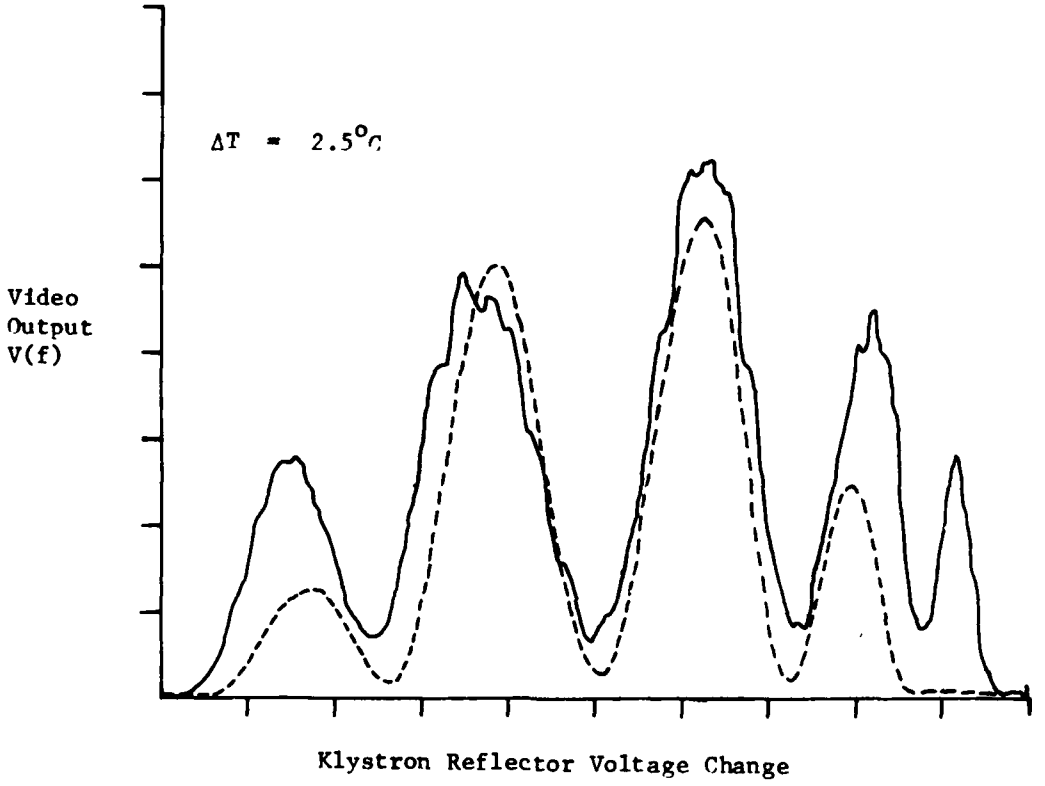

Figure 24. Simulation: two reflectors separated by 4 meters.

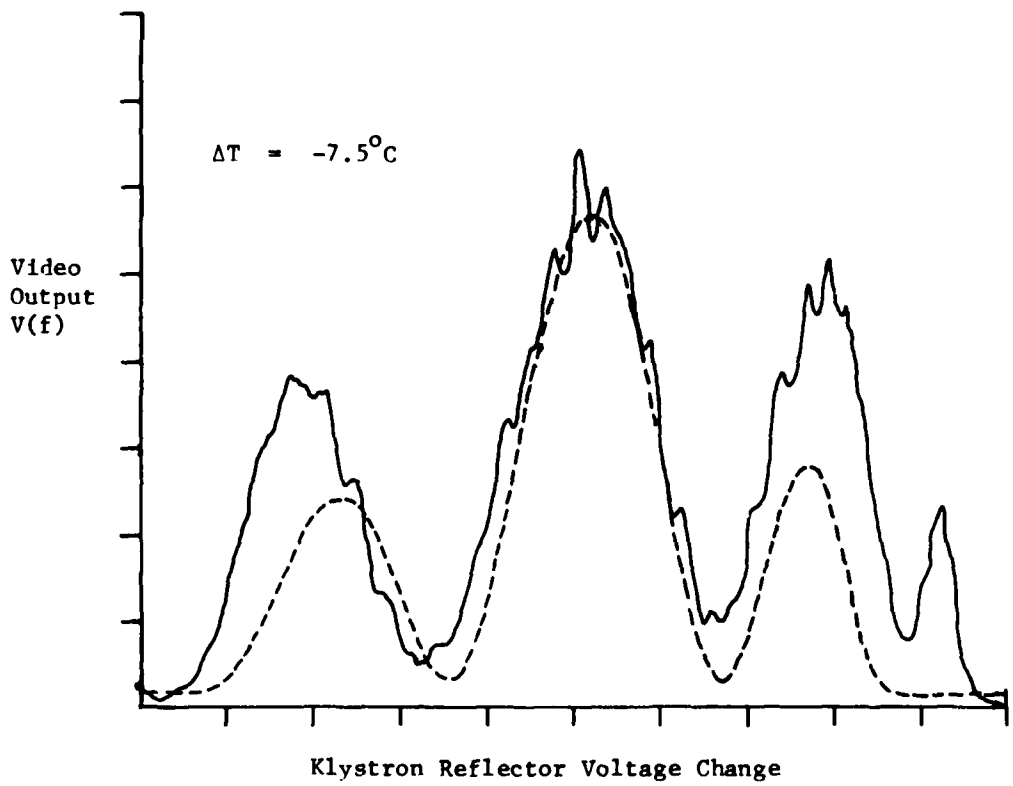

Figure 25. Simulation: two reflectors separated by 3 meters.

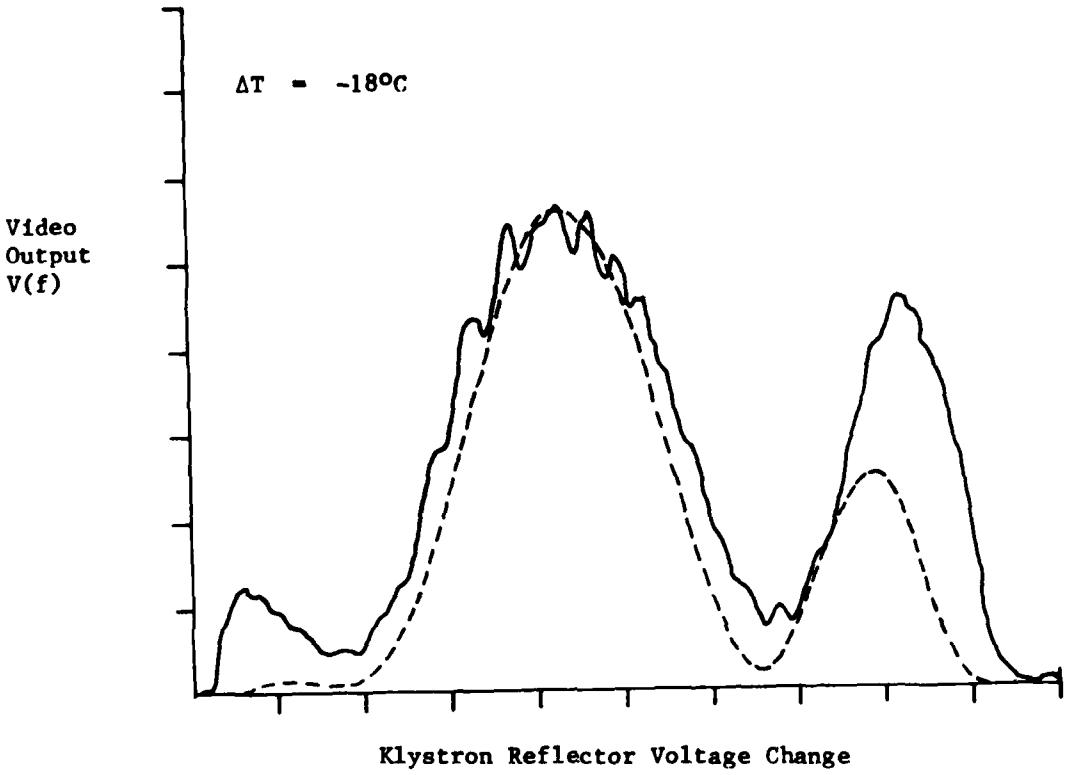

Figure 26. Simulation: two reflectors separated by 2 meters.

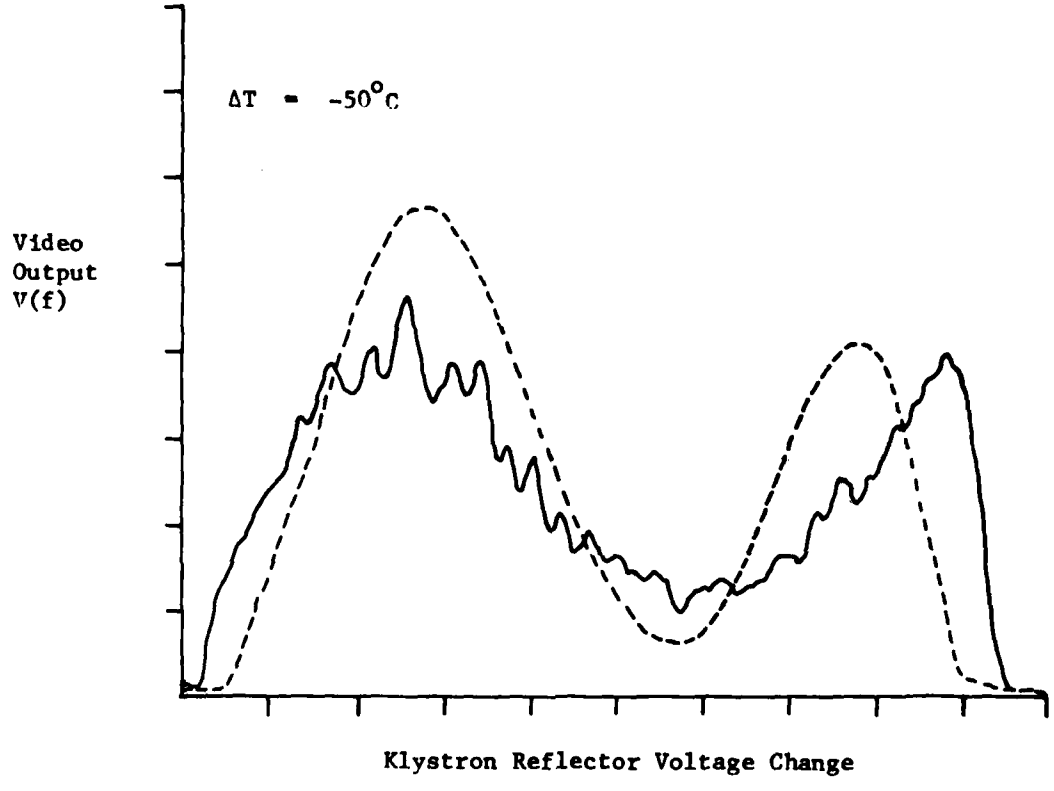

Figure 27. Simulation: two reflectors separated by 1 meter.

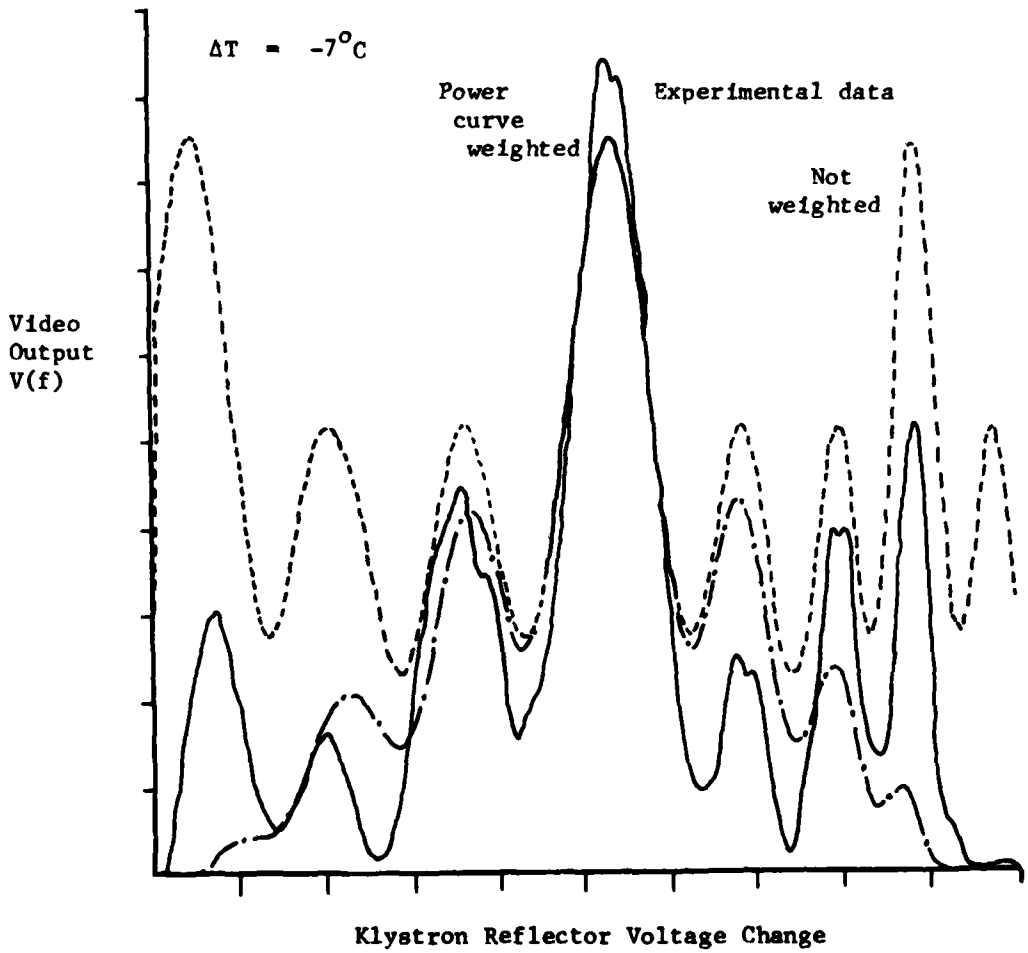

Figure 28. Simulation: three reflectors separated by 4m, 2m.

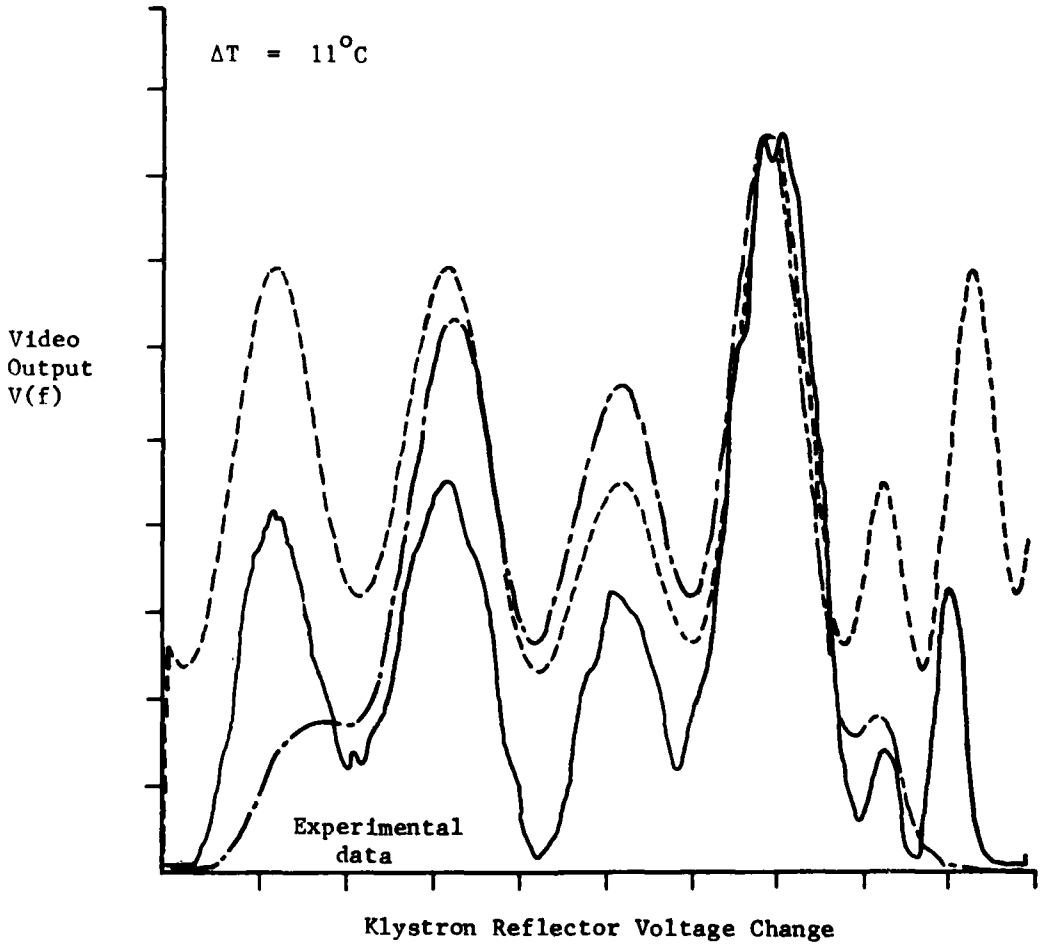

Figure 29. Simulation: three reflectors separated by 3m, 2m.

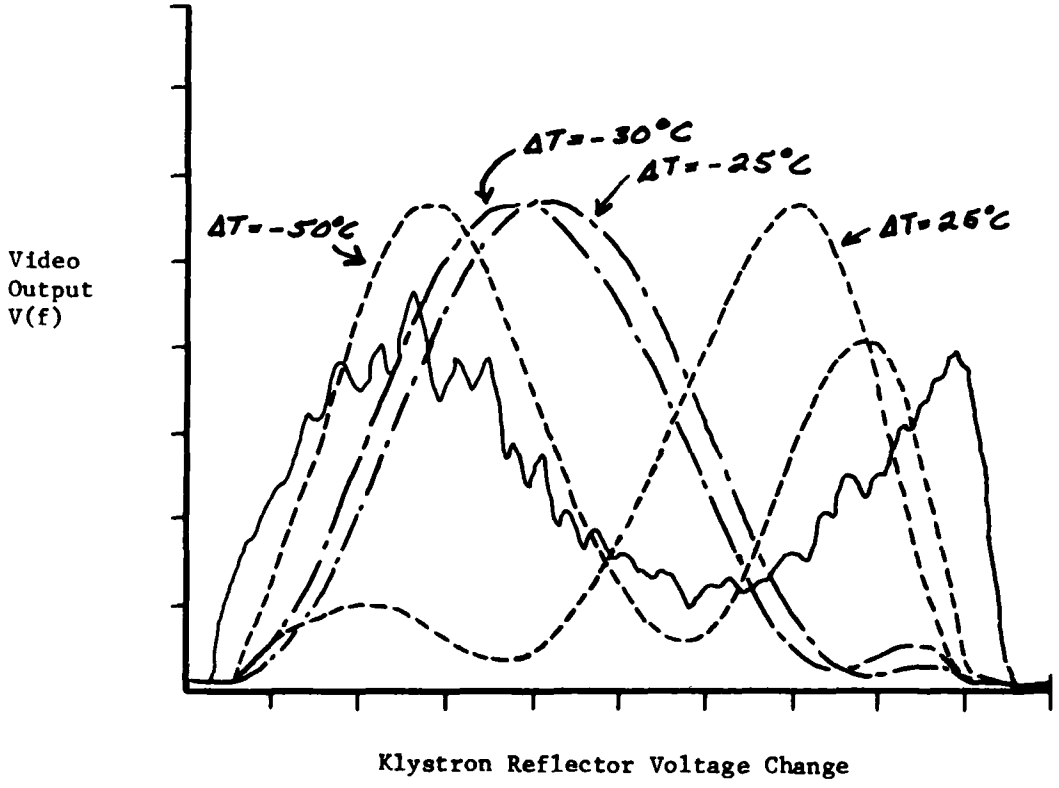

Figure 30. Simulation: two reflectors separated by 1 meter - temperature effects.

resulting in a decrease in the period of the oscillation after the reflector voltage change reaches 60 units. This effect has been accurately modeled in the simulation by plotting the results as a function of reflector voltage change, rather than as a function of frequency. Only when the frequency curve is perfectly linear can the experimental data be considered to be an amplitude versus frequency plot.

Figure 31 shows the output of the FFT for the data produced by the simulation for a separation between reflectors of 6 meters. As noted in the figure, the result is for a flat power spectrum and a perfectly linear sweep of the source. Figures 32 and 33 show the results of the FFT of the data produced by the simulation for the other cases of interest. All of the plots are normalized to the largest coefficient (dc term) of the FFT. Figures 34 through 36 display the same cases for a separation of 4 meters.

Figures 37 and 38 provide the results of FFT's of the simulated data for the three reflector case without and with degradation. Figure 38 can then be compared to Figure 39, which is an FFT of the experimental data obtained by manually digitizing the data and calculating the spectrum. Figure 40 shows the results for experimental data for separations of 3 meters, 2 meters. The FFT of the actual data displays a broader and, hence, flatter spectrum that the FFT of the simulation result. The combined effect of the nonlinear power curve and nonlinear frequency sweep is to spread the power over the range domain. These effects combine to mask the expected range separation lines and introduce others which make the target appear more complicated.

VII. CONCLUSIONS AND RECOMMENDATIONS

For the data collected with two corner reflectors, there is excellent agreement between the measured range separations and those calculated from the radar results. There is, in general, good qualitative agreement between the experimental interference patterns and those obtained from theoretical computer simulation for both two reflector and three reflector data.

Most of the temperature shifts required to adjust the phase of the interference pattern (or, equivalently, to adjust the frequency span end points) are not unreasonable. The temperature in the High Bay during the experiment was low (~10°C), while the surface body temperature of the klystron during normal operation is probably higher than 50°C. In order to conserve tube lifetime, the klystron was often turned off between measurements, occasionally for long periods of time. Thus, large temperature variations were possible.

In addition, some phase change may be due to regulation or inadvertent adjustment of the klystron beam (resonator) voltage. An increase in beam voltage causes a decrease in frequency; a crude measurement indicated a sensitivity on the order of -1 MHz/V.

Two factors contributed to the discrepancies between the theoretical and experimental interference patterns with respect to amplitudes: (1) the inability to adequately characterize the power curve (note: actually the power curve used should have been the interference pattern obtained with only one reflector, since receiver characteristics are also included); and (2) because the antenna beamwidths were so narrow, the unlikelihood that the corner

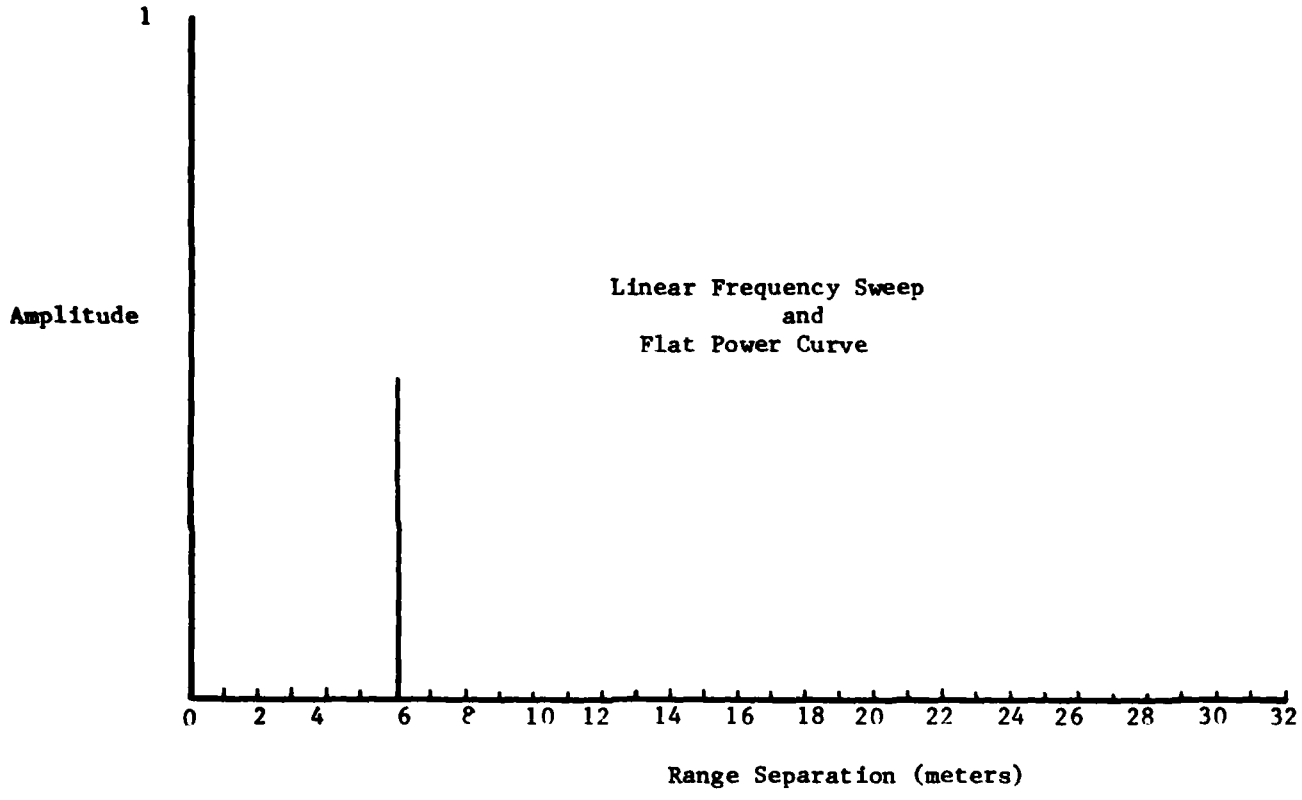

Figure 31. FFT for two reflectors separated by 6 meters.

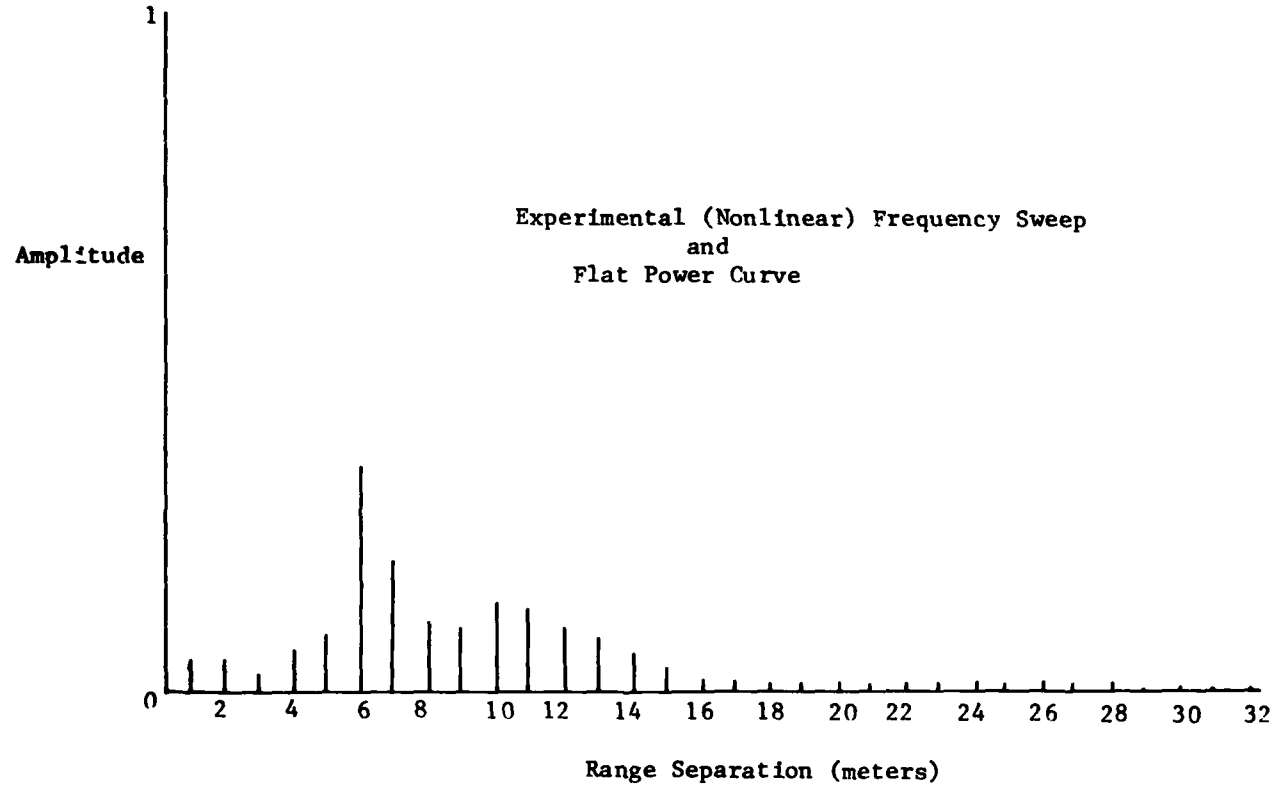

Figures 32. Degraded FFT for two reflectors separated by 6 meters.

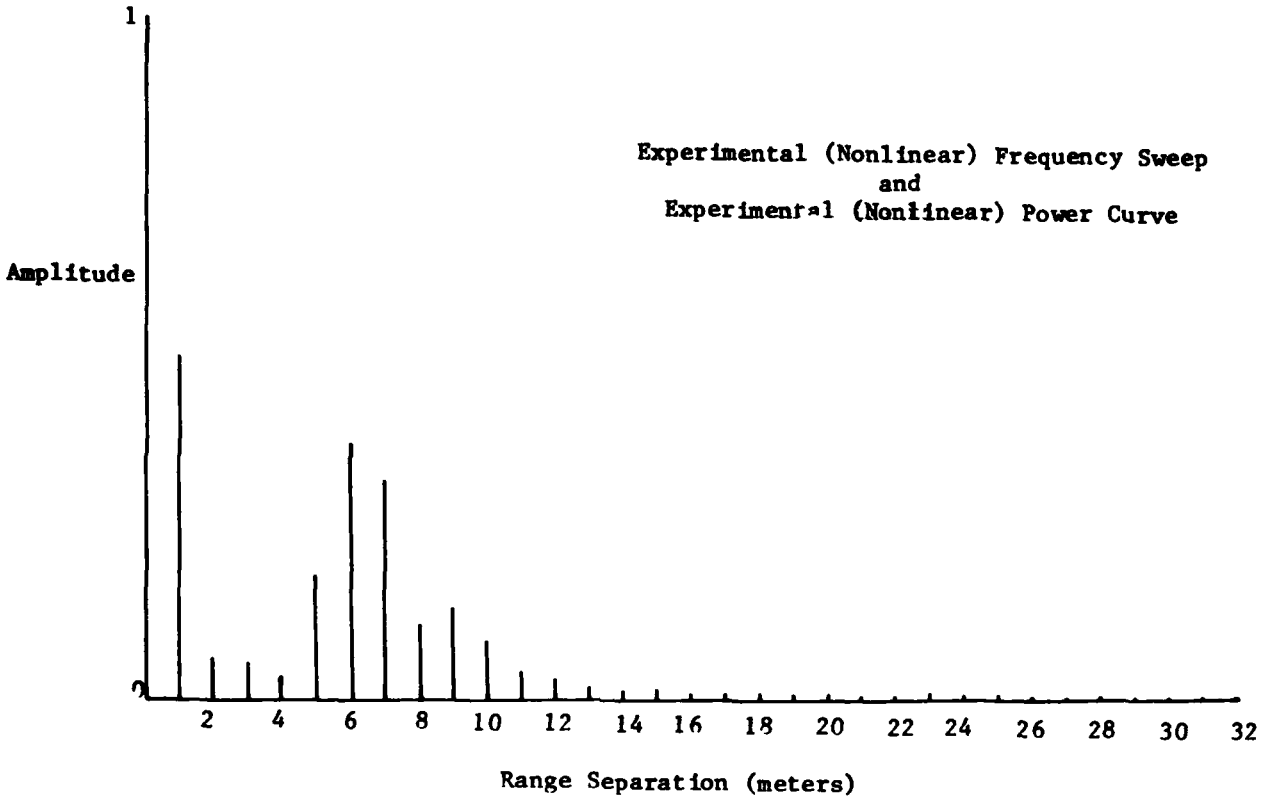

Figure 33. Further degraded FFT for two reflectors separated by 6 meters.

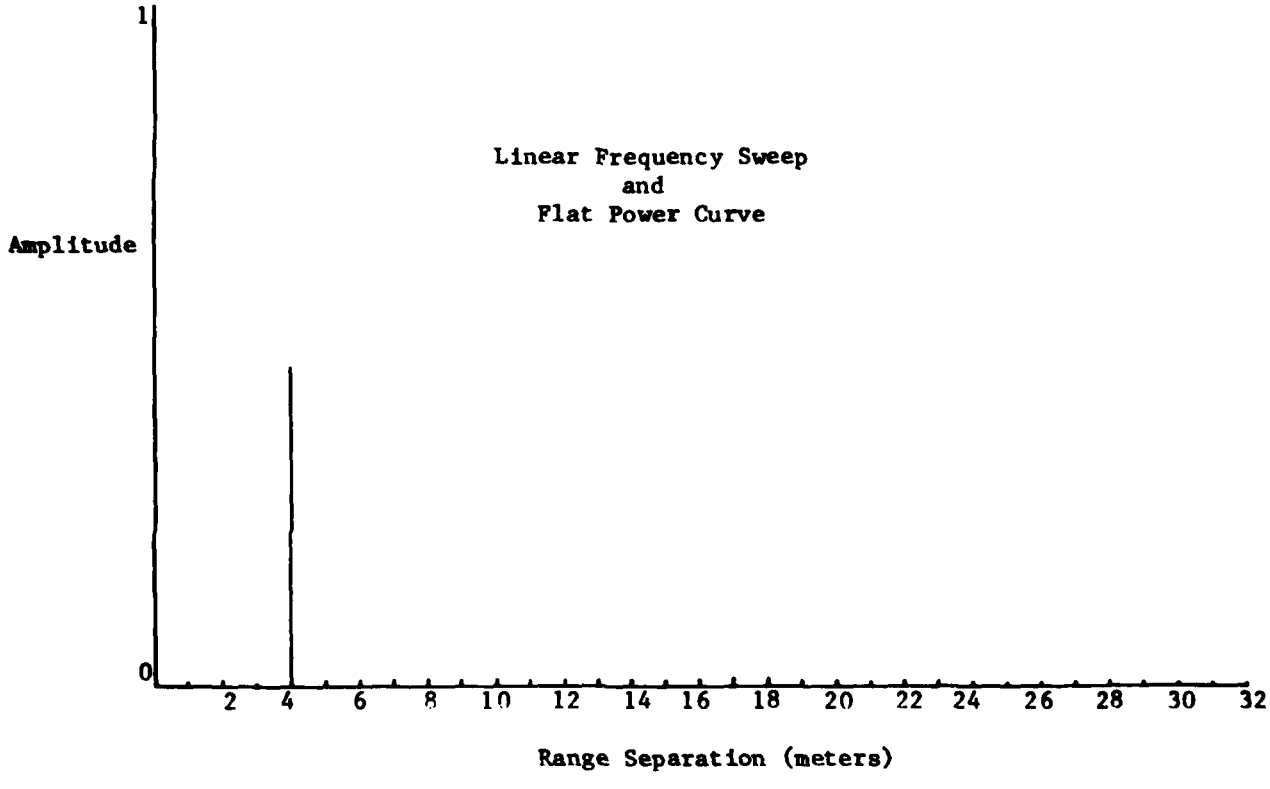

Figure 34. FFT for two reflectors separated by 4 meters.

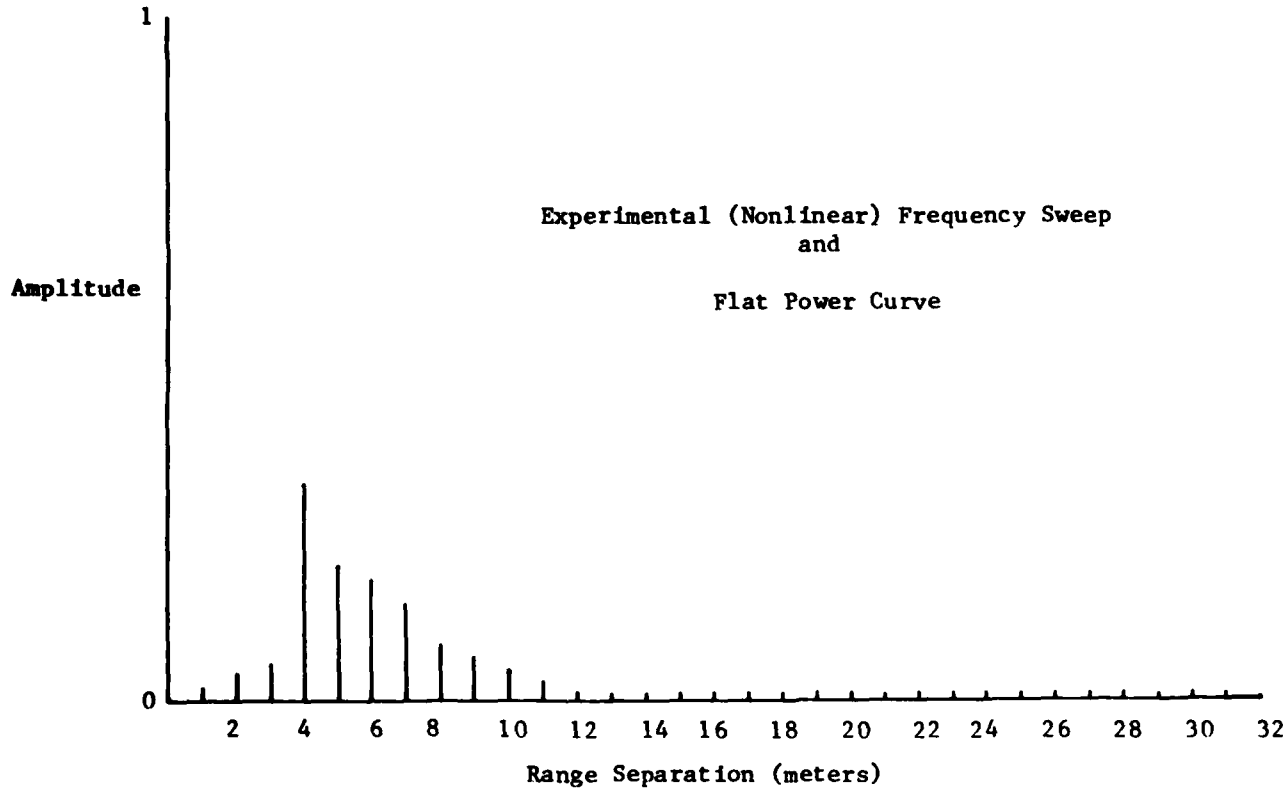

Figure 35. Degraded FFT for two reflectors separated by 4 meters.

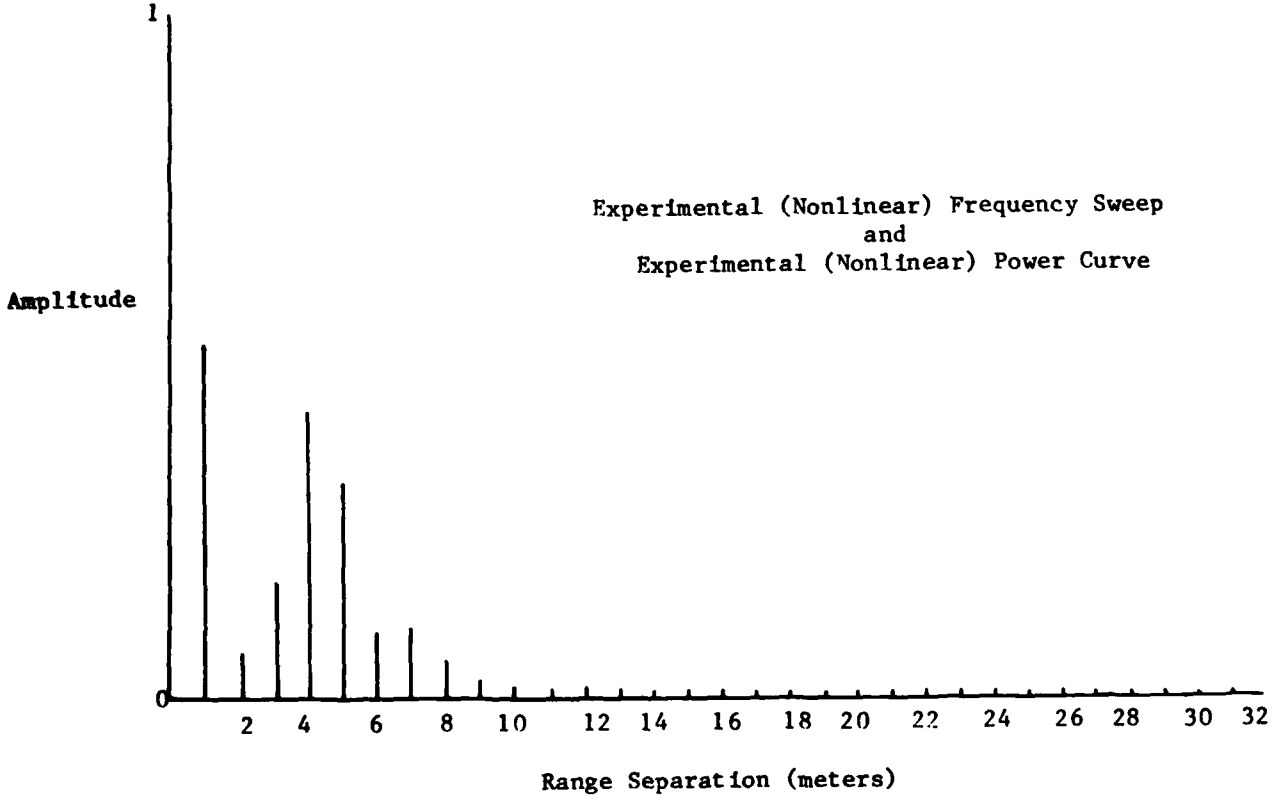

Figure 36. Further degraded FFT for two reflectors separated by 4 meters.

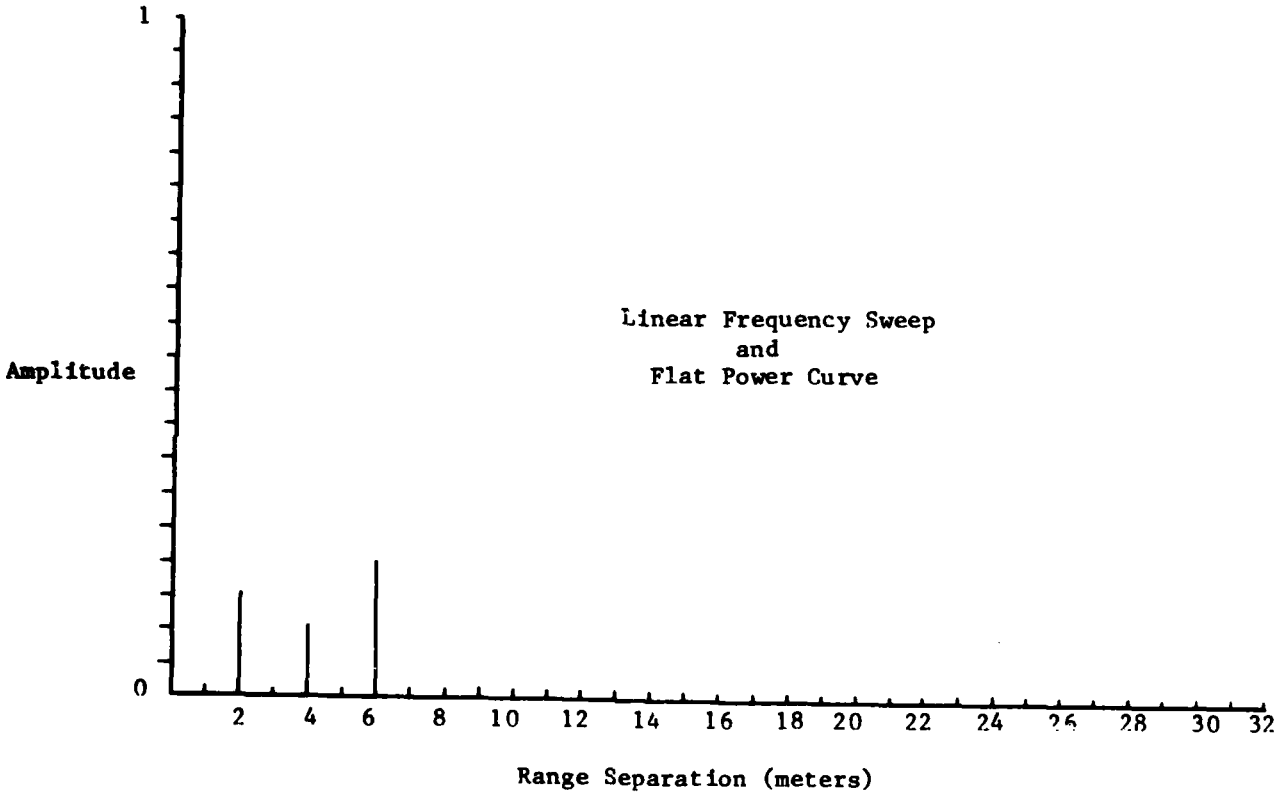

Figure 37. FFT for three reflectors separated by 4m, 2m.

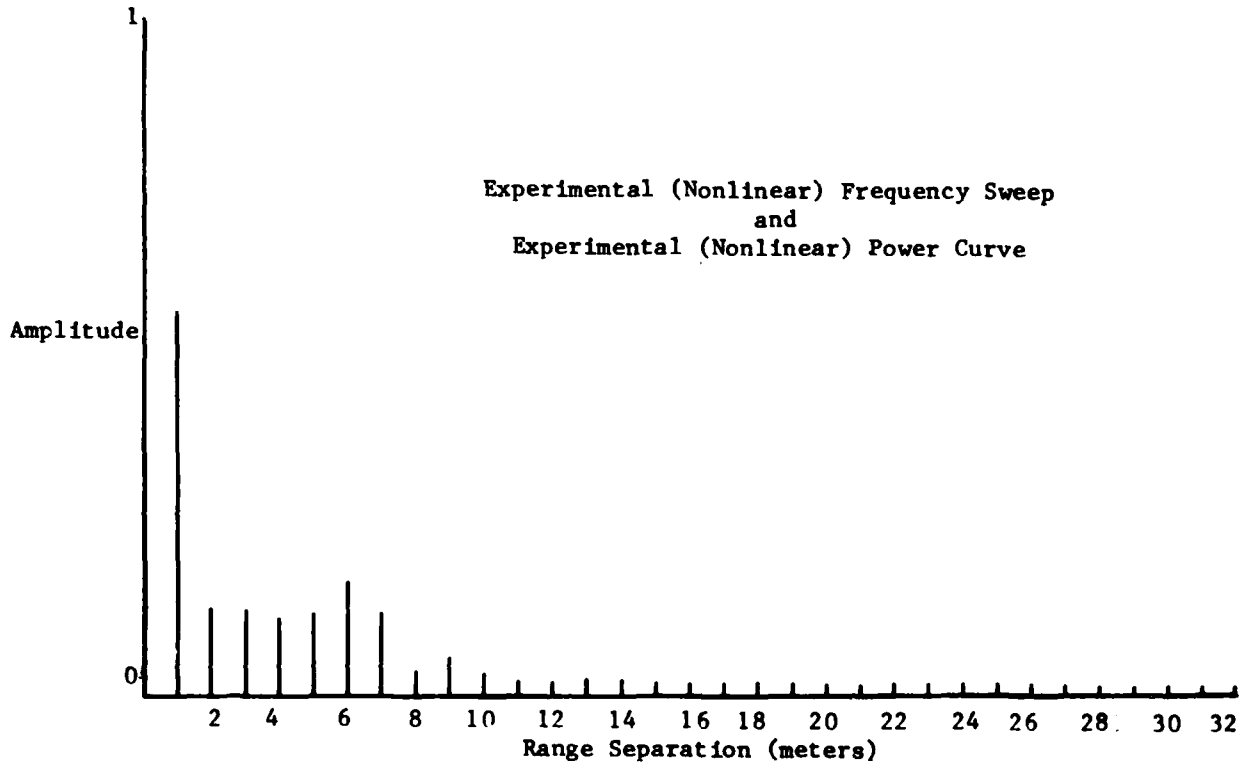

Figure 38. Degraded FFT for three reflectors separated by 4m, 2m.

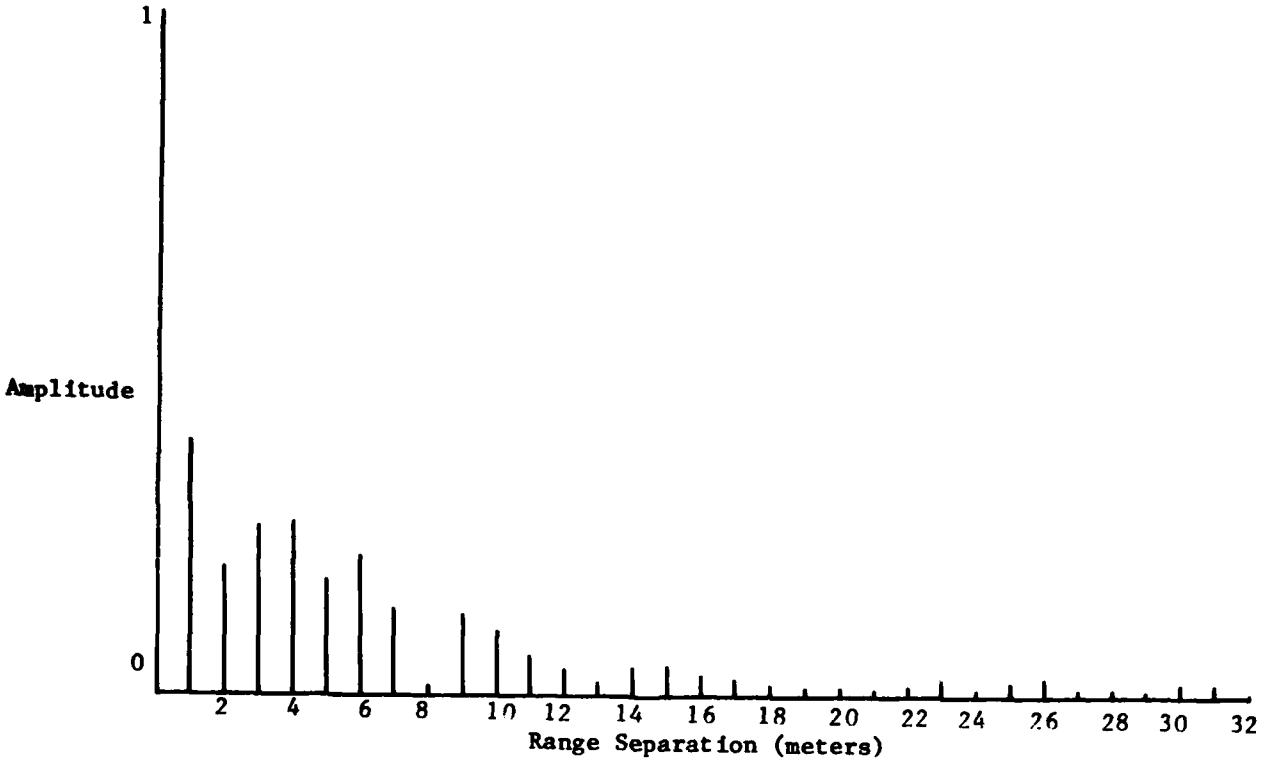

Figure 39. FFT of experimental data for three reflectors separated by 4m, 2m.

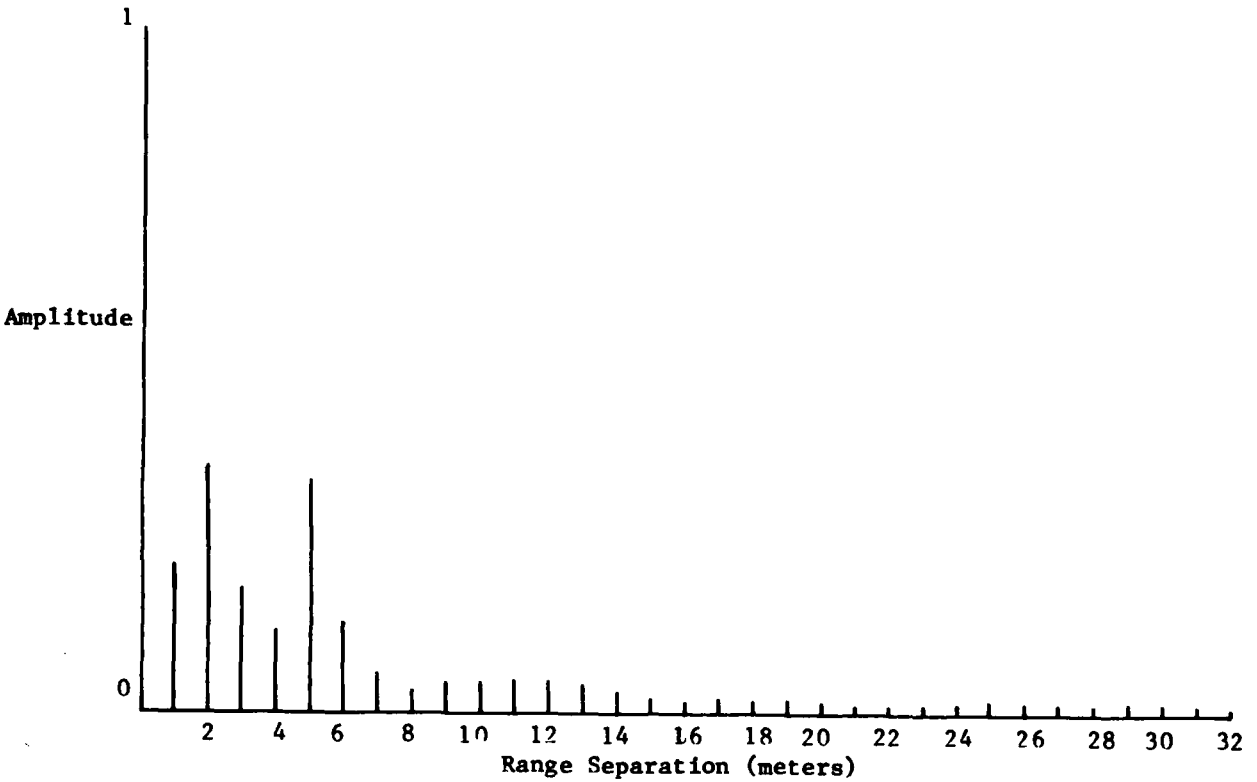

Figure 40. FFT of experimental data for three reflectors separated by 3m, 2m.

reflectors were equally illuminated by the transmit antenna or equally subtended by the receive antenna (especially for the measurements with three reflectors). Discrepancies with respect to the positions of maxima and minima along the "klystron reflector voltage change" axis result from the inability to adequately obtain the klystron frequency dependence on reflector voltage; spectrum analysis is required.

The agreement between the Fourier transform experimental and theoretical data is less apparent, again, due to the problems cited above. Such agreement is critical if the sensor is to be used to investigate complex targets. The fine structure in the experimental data show up as spectral lines which indicate wide range separations.

It is evident that the basic radar measurement, i.e., the interference pattern, contains target information greatly modified by the dynamic sensor characteristics. In order that the data are more representative of the target than of the radar, the following radar attributes are deemed desirable:

1. The frequency of the source should be a linear function of the control voltage, or the control voltage be such that the frequency sweep is linear, and that a voltage proportional to frequency be provided.

2. The transmitted and received power curve should be flat over the frequency diverse bandwidth, or it should be adequately characterized and allowances made for it in signal processing; this requirement is increasingly more critical for increasingly more complex targets.

3. The frequency diverse bandwidth should be as large as possible.

4. The transmitter and receiver should be temperature controlled, or their temperature characteristics should be determined over the operating ranges and compensated for. Note that a phase change in the interference pattern does not affect the Fourier transformed data, provided that the bandwidth is sufficiently large.

5. A pulsed system is preferable to a continuous wave system, in order to limit the effects of clutter (such as occurred, as a result of the High Bay door). Pulse width can be adjusted to maximize target response while minimizing clutter contamination. Pulse-to-pulse coherence is not required.

In terms of bandwidth, temperature effects, power curve and frequency nonlinearities, and continuous wave operation, the 94 GHz reflex klystron is clearly not an adequate source for application to complex targets. The radar at 140 GHz had a reasonable bandwidth, but also had severely nonlinear power characteristics. It is recommended, therefore, that further research be performed in an effort to find suitable millimeter wave sources and to build and test experimental systems achieving the desirable characteristics delineated.

Three millimeter wave (near 3mm) sources are currently available which have large electronically tuned frequency diverse bandwidths. The first, a 94 GHz solid state source employing a varactor controlled gunn diode oscillator, has a bandwidth of 600 MHz with a continuous wave power output of 30mW. Although this power level is probably too low for tactical systems, the device is coherent, and pulse compression may be employed. The cost is about $16 k.

The second source is a 80 GHz rising sun magnetron tube having a 3-4 kilowatt peak power output and a 1 GHz agile bandwidth. Rapid tuning is achieved by movement of a small conducting ring at one end of a rising sun resonant cavity. The tuning ring is supported and moved by a piezoelectric transducer. The magnetron pulse duration is typically 50 ns with a duty cycle of 0.0002. A high voltage power supply (100kW) is required. The cost of the tube is only about $20 k.

The third off-the-shelf source is an O-type backward-wave oscillator (carcinotron), electronically tunable from 88 GHz to 92 GHz. Continuous wave power over this bandwidth is 0.3 to 4 watts, although higher power can be achieved with narrower bandwidths. Tube cost is $20-25 k. Kilovolt power supplies are required.

In addition, there is in developement a 94 GHz coupled cavity traveling wave tube (TWT) with a 2 GHz bandwidth. Power output is 100W with a 0.50 duty cycle.

APPENDIX A

```
1 REM THIS PROGRAM WILL SIMULATE A FREQUENCY DIVERSE RADAR WHOSE SIGNAL
2 REM IS THE INPUT TO A SQUARE LAW DETECTOR.  THE OUTPUT OF THE PROGRAM
3 REM IS THE DETECTED OUTPUT OF THE SQUARE LAW DETECTOR.
10 DIM W[256],S[25],R[25],A[100]
20 DIM F[100],G[256],C[256],X[256]
40 DISP "NUMBER OF SCATTERS=";
50 INPUT N
60 DISP "ENTER # OF STEPS";
70 INPUT N1
80 DISP "ENTER TEMP CHANGE(C)";
90 INPUT C1
120 FOR I=1 TO 21
130 READ A[I]
140 NEXT I
150 FOR I=1 TO 21
160 READ F[I]
170 NEXT I
180 FOR L=1 TO N
190 DISP "ENTER RCS FOR EACH SCATTER";
200 DISP L;
210 INPUT S[L]
220 DISP "ENTER RANGE(M) TO THE SCATTERER";
230 DISP L;
240 INPUT R[L]
250 NEXT L
260 FOR K=1 TO N1
270 Z=(K-1)/(N1/20)
280 Z1=Z-INT(Z)
290 IF Z1<1E-06 THEN 330
300 G[K]=(F[INT(Z)+2]-F[INT(Z)+1])*Z1+F[INT(Z)+1]+((-1.6E+06)*C1)
310 C[K]=(A[INT(Z)+2]-A[INT(Z)+1])*Z1+A[INT(Z)+1]
320 GOTO 350
330 G[K]=F[INT(Z)+1]+(-1.6E+06*C1)
340 C[K]=A[INT(Z)+1]
350 V1=0
```

```
360 FOR I=1 TO (N-1)
370 FOR J=(I+1) TO N
380 R1=R[J]-R[I]
390 C=3E+08
400 A1=4*PI*G[K]*(R1/C)
410 B=(C[K])*(S[I]+S[J]+2*SQR(S[I]*S[J])*COS(A1))
420 V1=V1+B
430 NEXT J
440 NEXT I
450 V[K]=V1
460 IF K>1 THEN 490
470 V3=V[K]
480 GOTO 510
490 IF V[K]<V3 THEN 510
500 V3=V[K]
510 NEXT K
520 SCALE 0,N1,0,1
530 FOR K=1 TO N1
540 PLOT K,V[K]/V3,+0
550 NEXT K
560 STOP
570 DATA 0,0,0.1,0.21,0.375,0.53,0.67,0.785,0.875,0.935,0.98,0.99,0.95,0.88
580 DATA 0.765,0.595,0.4,0.18,0.01,0,0
590 DATA 9.3958E+10,9.39655E+10,9.39735E+10,9.39825E+10,9.399E+10,9.3997E+10
600 DATA 9.4005E+10,9.4013E+10,9.4021E+10,9.40285E+10,9.4035E+10,9.40425E+10
610 DATA 9.405E+10,9.4059E+10,9.4069E+10,9.4079E+10,9.40905E+10,9.41055E+10
620 DATA 9.412E+10,9.41345E+10,9.4149E+10
1500 END
```

APPENDIX B

```
2041 REM THIS PROGRAM WILL TAKE A N POINT DFT OF AN INPUT DATA ARRAY V(I)
2042 REM THE DATA ARRAY MUST BE REAL.  THE NUMBER OF DATA POINTS MUST A POWER
2043 REM  OF 2, NOT TO EXCEED 8 (256 POINTS). THIS PROGRAM ASSUMES THAT ALL
2044 REM ARRAYS ARE DIMENSIONED IN THE CALLING PROGRAM.
2045 REM THIS IS AN IN PLACE FFT. THE ELEMENTS OF DATA (V(I)) ARE REPLACED
2046 REM BY THE FFT COEFFICIENTS.
2050 N2=N1/2
2060 N3=N1-1
2070 J=1
2090 REM G(I)=REAL PART OF V(I)
2100 REM C(I) = IMAGINARY PART OF V(I)
2110 FOR I=1 TO N1
2120 C[I]=0
2130 G[I]=V[I]
2140 NEXT I
2141 GOSUB 2570
2150 REM THE ABOVE STATEMENTS INITIALIZE Y(I) & Z(I)
2160 REM THE # OF POINTS MUST SATISFY N=2↑M
2170 DISP "INPUT M";
2180 INPUT M
2190 X1=0
2200 FOR L=1 TO M
2210 L2=INT(2↑L)
2220 L3=INT(L2/2)
2230 U1=1
2240 U2=0
2250 W1=COS(PI/L3)
2260 W2=SIN(PI/L3)
2270 FOR J=1 TO L3
2280 FOR I=J TO N1 STEP L2
2290 I1=INT(I+L3)
2300 T1=(G[I1]*U1)-(C[I1]*U2)
2310 T2=(G[I1]*U2)+(C[I1]*U1)
2320 G[I1]=G[I]-T1
2330 C[I1]=C[I]-T2
2340 G[I]=G[I]+T1
2350 C[I]=C[I]+T2
2370 NEXT I
```

```
2371 D=U1
2372 D1=U2
2380 U1=(D*W1)-(D1*W2)
2390 U2=(D*W2)+(D1*W1)
2400 NEXT J
2410 NEXT L
2420 FOR I=1 TO N1
2430 X[I]=SQR((G[I]↑2)+(C[I]↑2))
2440 IF X[I]<X1 THEN 2460
2450 X1=X[I]
2460 NEXT I
2480 SCALE 0,N1,0,1
2490 FOR I=1 TO N1+1
2500 PLOT I-1,X[I]/X1,+2
2501 IPLOT 1,-X[I]/X1,+1
2510 NEXT I
2520 STOP
2570 FOR I=1 TO N3
2580 IF I >= J THEN 2620
2590 T1=G[J]
2600 G[J]=G[I]
2610 G[I]=T1
2620 K=N2
2630 IF K >= J THEN 2670
2640 J=J-K
2650 K=K/2
2660 GOTO 2630
2670 J=J+K
2680 NEXT I
2690 RETURN
2700 END
```

APPENDIX C

```
10 DIM V[256],S[25],R[25],A[100]
20 DIM F[100],G[256],C[256],X[256]
40 DISP "NUMBER OF SCATTERS=";
50 INPUT N
80 DISP "ENTER TEMP CHANGE(C)";
90 INPUT C1
120 FOR I=1 TO 21
130 READ A[I]
140 NEXT I
150 FOR I=1 TO 21
160 READ F[I]
170 NEXT I
171 DISP "ENTER # OF STEPS";
172 INPUT N1
180 FOR L=1 TO N
190 DISP "ENTER RCS FOR EACH SCATTER";
200 DISP L;
210 INPUT S[L]
220 DISP "ENTER RANGE(M) TO THE SCATTERER";
230 DISP L;
240 INPUT R[L]
250 NEXT L
260 FOR K=1 TO N1
270 Z=(K-1)/(N1/20)
280 Z1=Z-INT(Z)
290 IF Z1<1E-06 THEN 330
300 G[K]=(F[INT(Z)+2]-F[INT(Z)+1])*Z1+F[INT(Z)+1]+((-1.6E+06)*C1)
310 C[K]=(A[INT(Z)+2]-A[INT(Z)+1])*Z1+A[INT(Z)+1]
320 GOTO 350
330 G[K]=F[INT(Z)+1]+(-1.6E+06*C1)
340 C[K]=A[INT(Z)+1]
350 V1=0
```

```
360 FOR I=1 TO (N-1)
370 FOR J=(I+1) TO N
380 R1=R[J]-R[I]
390 C=3E+08
400 A1=4*PI*G[K]*(R1/C)
410 B=(C[K])+(S[I]+S[J]+2*SQR(S[I]*S[J])*COS(A1))
420 V1=V1+B
430 NEXT J
440 NEXT I
450 V[K]=V1
460 IF K>1 THEN 490
470 V3=V[K]
480 GOTO 510
490 IF V[K]<V3 THEN 510
500 V3=V[K]
510 NEXT K
511 GOTO 560
520 SCALE 0,N1,0,1
530 FOR K=1 TO N1
540 PLOT K,V[K]/V3,+0
550 NEXT K
560 STOP
570 DATA 0,0,0.1,0.21,0.375,0.53,0.67,0.785,0.875,0.935,0.98,0.99,0.95,0.88
580 DATA 0.765,0.595,0.4,0.18,0.01,0,0
590 DATA 9.3958E+10,9.39655E+10,9.39735E+10,9.39825E+10,9.399E+10,9.3997E+10
600 DATA 9.4005E+10,9.4013E+10,9.4021E+10,9.40285E+10,9.4035E+10,9.40425E+10
610 DATA 9.405E+10,9.4059E+10,9.4069E+10,9.4079E+10,9.40905E+10,9.41055E+10
620 DATA 9.412E+10,9.41345E+10,9.4149E+10
630 LINK 2,640
640 N2=N1/2
650 N3=N1-1
660 J=1
680 REM G(I)=REAL PART OF V(I)
690 REM C(I) = IMAGINARY PART OF V(I)
700 FOR I=1 TO N1
710 C[I]=0
720 G[I]=V[I]
730 NEXT I
731 GOSUB 1160
740 REM THE ABOVE STATEMENTS INITIALIZE Y(I) & Z(I)
750 REM THE # OF POINTS MUST SATISFY N=2↑M
760 DISP "INPUT M";
770 INPUT M
780 X1=0
790 FOR L=1 TO M
800 L2=INT(2↑L)
```

```
 810 L3=TU* L2/2
 820 U1=1
 830 U2=0
 840 W1=COS(PI/L3)
 850 W2=SIN(PI/L3)
 860 FOR J=1 TO L3
 870 FOR I=J TO N1 STEP L2
 880 I1=INT(I+L3)
 890 T1=(G[I1]*U1)-(C[I1]*U2)
 900 T2=(G[I1]*U2)+(C[I1]*U1)
 910 G[I1]=G[I]-T1
 920 C[I1]=C[I]-T2
 930 G[I]=G[I]+T1
 940 C[I]=C[I]+T2
 960 NEXT I
 961 D=U1
 962 D1=U2
 970 U1=(D*W1)-(D1*W2)
 980 U2=(D*W2)+(D1*W1)
 990 NEXT J
1000 NEXT L
1010 FOR I=1 TO N1
1020 X[I]=SQR((G[I]↑2)+(C[I]↑2))
1030 IF X[I]<X1 THEN 1050
1040 X1=X[I]
1050 NEXT I
1070 SCALE 0,N1/2,0,1
1080 FOR I=1 TO N1/2
1090 PLOT I-1,X[I]/X1,+2
1091 IPLOT 1,-X[I]/X1,+1
1100 NEXT I
1110 STOP
1160 FOR I=1 TO N3
1170 IF I >= J THEN 1210
1180 T1=G[J]
1190 G[J]=G[I]
1200 G[I]=T1
1210 K=N2
1220 IF K >= J THEN 1260
1230 J=J-K
1240 K=K/2
1250 GOTO 1220
1260 J=J+K
1270 NEXT I
1280 RETURN
1290 END
```

REFERENCES

1. N. Backmark, J. E. Krim, and F. Sellberg, "Frequency-Agile Radar," Philips Technical Review, Volume 28, 1967, pp. 323-238.

2. V. G. Hansen, "A Sequential Logic for Improving Signal Detectability in Frequency-Agile Search Radars," IEEE Trans. Aerosp. Electron. Syst., Volume AES-4, September 1968, pp. 763-773.

3. G. Grasso and P. F. Guarguaglina, "General Detection Procedure for a Multifrequency Radar," Alta Frequenza, Volume XXXVII, February 1968, pp. 132-138.

4. V. Vannicola, "Detection of Slow Fluctuating Targets with Frequency Diversity Channels," IEEE Trans. Aerosp. Electron. Syst., Volume AES-10, January 1974, pp. 43-52.

5. W. P. Birkmeier and N. D. Wallace, "Radar Tracking Accuracy Improvement by Means of Pulse-to-Pulse Frequency Modulation," AIEE Trans. (Commun. Electron.), Volume 81, 1962, pp. 571-575 (January 1963 sec.).

6. G. Lind, "Reduction of Radar Tracking Errors with Frequency Agility," IEEE Trans. Aerosp. Electron. Syst., Volume AES-4, May 1968, pp. 410-416.

7. R. J. Sims and E. R. Graf, "The Reduction of Radar Glint by Diversity Techniques," IEEE Trans. Antennas Propagat., Volume Ap-19, July 1971, pp. 462-468.

8. K. Ruttenberg and L. Chanzit, "High Range Resolution by Means of Pulse-to-Pulse Frequency Shifting," EASCON '68 Record, 1968, pp. 47-51.

9. P.M. Alexander and J. L. Brown, "A Preliminary Assessment of Target Classification Using Noncoherent Radar Waveforms," US Army Missile Command, Technical Report T-79-80, July 1979.

10. L. M. Novak, "Stationary Target Acquisition: Modeling, Prediction, and Experimental Results (U)," presented at the 25th Annual Tri-Service Radar Symposium, Monterey, CA, 18-20 September 1979. (CONFIDENTIAL)

11. _____, "ARPA/TTO Program HOWLS (U)," Massachussetts Institute of Technology, Lincoln Laboraory, ESD-TR-79-218, July 1979. (CONFIDENTIAL)

12. L. M. Novak, "Millimeter Seeker Radar Target Acquisition Studies (U)," Proceedings of the Eighth DARPA/Tri-Service Millimeter Wave Conference, August 1979, pp. 469-487. (CONFIDENTIAL)

13. P. M. Alexander, "Frequency Diverse Tracking/Guidance Radar Adapted to Target Acquisition," Proceedings of the 1980 Army Science Conference, June 1980.

14. E. K. Reedy, J. L. Eaves, S. O. Piper, W. K. Parks, S. P. Brookshire, R. D. Wetherington, and R. N. Trevits, Stationary Target Detection and Classification Studies (U), US Army Electronics Command, Report ECOM-76-0961-2, March 1978. (CONFIDENTIAL)

15. D. J. Lewinski, J. D. Echard, E. O. Rausch, S. O. Piper, and J. L. Eaves, "Stationary Target Detection and Classification Studies," US Army Electronics Research and Development Command, Report DELCS-TR-76-0961-F, April 1979.

16. L. W. Root, Jr., and R. N. Cullis, "Multi-Environment Active RF Seeker (MARFS) (U)," Proceedings of the Seventh-DARPA/Tri-Service Millimeter Wave Conference, September 1978. (CONFIDENTIAL)

17. R. E. Stovall, "A Gaussian Noise Analysis of the 'Pseudo-Coherent Discriminant,'" Massachussetts Institute of Technology, Lincoln Laboratory, Technical Note 1978-46, December 1978.

18. P. M. Alexander, "A Mathematical Analysis of Polarimetric Phase and Amplitude with Frequency Agility for Radar Target Acquisition," US Army Missile Command, Technical Report, T-79-92, September 1979.

19. M. C. Schexnayder, H. M. Grass, and P. M. Alexander, "Initial Test of 140 GHz Coherent Radar for Millimeter Beamrider Guidance," US Army Missile Command, Internal Technical Note, RE-80-5, January 1980.

20. S. Y. Liao, Microwave Devices and Circuits, Englewood Cliffs, NJ, Prentice-Hall, Inc., 1980, Chapter 5, p. 204.

DISTRIBUTION LIST

	No. of Copies
IIT Research Institute Guidance and Control Information and Analysis Center (GACIAC) 10 West 35th Street Chicago, IL 60616	1
Commander US Army Material Systems Analysis Activity ATTN: DRXSY-MP Aberdeen Proving Ground, MD 21005	1
Commander US Materiel Development and Readiness Command 5001 Eisenhower Avenue Alexandria, VA 22333	1
Commander Defense Advanced Research Projects Agency 1400 Wilson Boulevard Arlington, VA 22209	1
Commander US Army Research Office PO Box 12211 Research Triangle Park, NC 27709	1
Commander US Army Armament R&D Command Picatinny Arsenal, Dover, NJ 07801	1
Commander US Army Armament R&D Command Ballistic Research Laboratories Aberdeen Proving Ground, MD 21005	1
Commander US Army Aviation R&D Command PO Box 209 St. Louis, MO 63166	1
Commander US Army Electronics R&D Command Atmospheric Sciences Laboratory White Sands Missile Range, NM 88002	1

DISTRIBUTION (Continued)

	No. of Copies
Commander US Army Electronics R&D Command US Army Electronic Warfare Laboratory Ft. Monmouth, NJ 07703	1
Commander US Army Electronics R&D Command Office of Missile Electronic Warfare White Sands Missile Range, NM 88022	1
Commander US Army Electronics R&D Command Combat Surveillance and Target Acquisition Laboratory Ft. Monmouth, NJ 07703	1
Commander US Army Electronics R&D Command Electronic Warfare Laboratory Ft. Monmouth, NJ 07703	1
Commander US Army Electronics R&D Command Electronics Technology and Devices Laboratory Ft. Monmouth, NJ 07703	1
Commander US Army Electronics R&D Command Night Vision and Electro-Optics Laboratory Ft. Belvoir, VA 22060	1
Commander US Army Electronics R&D Command Harry Diamond Laboratories 2800 Powder Mill Road Adelphi, MD 20783	1
Commander US Army Electronics R&D Command Project Manager, SOTAS Ft. Monmouth, NJ 07703	1
Commander US Army Mobility Equipment R&D Command Ft. Belvoir, VA 22060	1
Commander US Army Air Mobility Research and Development Laboratory AMES Research Center Moffett Field, CA 94035	1

DISTRIBUTION (Continued)

	No. of Copies
Commander US Army Tank-Automotive Command Warren, MI 48090	1
Commander US Army Missile Command Ballistic Missile Defense Advanced Technology Center PO Box 1500 Huntsville, AL 35807	1
Commander US Naval Research laboratory ATTN: Code 5300, Radar Division Washington, DC 20390	1
Commander US Naval Air Development Center Sensors & Avionics Technology Directorate Radar Division/Tactical Radar Branch Warminster, PA 18974	1
Commander US Naval Electronics Laboratory Center San Diego, CA 92152	1
Commander US Naval Surface Weapons Center Dahlgren, VA 22448	1
Commander US Naval Surface Weapons Center White Oak Laboratory Silver Spring, MD 20910	1
Commander US Naval Weapons Center China Lake, CA 93555	1
Commander US Air Force Systems Command US Air Force Armament Laboratory Eglin Air Force Base, FL 32542	1
Commander US Air Force Systems Command US Air Force Avionics Laboratory Wright-Patterson Air Force Base, OH 45433	1

DISTRIBUTION (Continued)

	No. of Copies
Commander US Air Force Systems Command Air Force Cambridge Research Laboratories Hanscom Air Force Base, MA 01731	1
Commander US Air Force Systems Command Rome Air Development Center Griffiss Air Forc Base, NJ 13441	1
Director Division 8 MIT Lincoln Laboratory Lexington, MA 02173	1
Director Radar and Instrumentation Laboratory Engineering Experiment Station Georgia Institute of Technology Atlanta, GA 30332	1
Automation Industries, Inc. Vitro Laboratories Division 14000 Georgia Avenue Silver Spring, MD 20910	1
AIL Division Cutler-Hammer Deer Park Long Island, NY 11729	1
Bell Aerospace Textron, Inc. PO Box 1 Buffalo, NY 14240	1
Boeing Aerospace Company PO Box 1470 Huntsville, AL 35807	1
Emerson Electric Company Electronics and Space Division 8100 W. Florissant Avenue St. Louis, MO 63163	1
Environmental Research Institute of Michigan Radar and Optics Division PO Box 618 Ann Arbor, MI 41807	1

DISTRIBUTION (Continued)

	No. of Copies
Ford Aerospace & Communications Corporation Aeronutronics Division Ford Road Newport Beach, CA 92663	1
General Dynamics Suite 42, Holiday Center South Memorial Parkway Huntsville, AL 35801	1
Goodyear Aerospace Corporation Akron, OH 44315	1
Goodyear Aerospace Corporation Arizona Divison Litchfield Park, AZ 85340	1
Lockheed Missile & Space Company, Inc. 4800 Bradford Drive Huntsville, AL 35807	1
Honeywell, Inc. Defense Systems Division 2600 Ridgway Parkway Minneapolis, MN 55413	1
Hughes Aircraft Corporation Advanced Missile Systems Division Canoga Park, CA 91304	1
IBM Army Missile Programs Federal Systems Division 150 Sparkman Drive Huntsville, AL 38505	1
Intergraph Corporation PO Box 5183 Huntsville, AL 35805	1
Mark Resources Incorporated 4676 Admiralty Way Suite 303 Marina Del Rey, CA 90291	1
Martin Marietta Aerospace PO Box 6167 Huntsville, AL 35806	1

DISTRIBUTION (Continued)

	No. of Copies
McDonnell Douglas Astronautics Company 3322 South Memorial Parkway, Suite 122 Huntsville, AL 35801	1
MITRE Corporation 4305 Middlesex Turnpike Bedford, MA 01730	1
Norden Systems, Inc. 314 Norden Place Norwalk, CT 06856	1
Northrop Corporation Defense Systems Division 600 Hicks Road Rolling Meadows, IL 60008	1
Raytheon Company Equipment Development Laboratories 430 Boston Post Road Wayland, MA 01778	1
RCA Government and Commercial Systems 3322 S. Memorial Parkway Suite 41 Huntsville, AL 35801	1
Riverside Research Institute 80 West End Avenue New York, NY 10023	1
Rockwell International Missile Systems Division 3370 Miraloma Avenue PO Box 4182 Anaheim, CA 92803	1
Sperry Microwave Electronics PO Box 4648 Clearwater, FL 33518	1
Sperry Research Center 100 North Road Sudbury, MA 01776	1
SRI International 1611 North Kent Street Rosslyn Plaza Arlington, VA 22209	1

DISTRIBUTION (Continued)

	No. of Copies
Technology Service Corporation 2811 Wilshire Blvd Santa Monica, CA 90403	1
Teledyne Brown Engineering Cummings Research Park Huntsville, AL 35807	1
Teledyne Micronetics 7155 Mission Gorge Road San Diego, CA 92120	1
Texas Instruments, Incorporated ATTN: Advanced Weapons Program Mail Stop 390 PO Box 6015 Dallas, TX 75222	1
TRW Defense and Space Systems Group 303 Williams Avenue, Suite 1231 Huntsville, AL 38501	1
Commander US Army Electronics R&D Command ATTN: DELET-M, Mr. N. Wilson	1
DELCS-R, Mr. D. Foiani	1
Mr. W. Fishbein	1
Mr W. Johnson	1
Mr. E. Frost	1
Mr. T. Ewanizky Ft. Monmouth, NJ 07703	1
Director Defense Advanced Research Projects Agency ATTN: Dr. James Tegnelia 1400 Wilson Boulevard Arlington, VA 22209	1
Commander US Air Force Systems Command US Air Force Armament Laboratory ATTN: Major R. Salemme Eglin Air Force Base, FL 32542	1
Emerson Electric Company Electronics and Space Division ATTN: Mr. R. Hermann Mr. O. B. Mitchell 8100 W. Florissant St. Louis, MO 63136	1

DISTRIBUTION (Concluded)

	No. of Copies
Georgia Institute of Technology Engineering Experiment Station ATTN: Dr. Robert McMillan	
Dr. Robert Shackleford	1
Mr. James Gallager	1
347 Ferst Drive Atlanta, GA 30332	1
MIT Lincoln Laboratory Division 8 ATTN: Dr. Peter Tannenwald	
Dr. Harold Fetterman	1
Dr. Jerry Waldman	1
Lexington, MA 02173	1
Sperry Research Center ATTN: Dr. R. M. Barnes 100 North Road Sudbury, MA 01776	1
DRSMI-LP, Mr. Voight	1
DRSMI-R, Dr. McCorkle	1
DRSMI-R, COL Feist	1
DRSMI-RN, Dr. Dobbins	1
DRSMI-RE, Mr. Lindberg	1
DRSMI-RE, Mr. Todd	1
DRSMI-RE, Mr. Pittman	1
DRSMI-REM, Mr. Haraway	1
DRSMI-REO, Mr. Ducote	1
DRSMI-RER, Mr. Low	1
DRSMI-RES, Mr. French	1
DRSMI-REG, Mr. Root	1
DRSMI-REL, Mr. Mangus	1
DRSMI-REL, Dr. Emmons	1
DRSMI-REL, Mr. Green	1
DRSMI-REL, Dr. Alexander	1
DRSMI-REL, Mr. Barley	25
DRSMI-REL, Mr. Grass	1
DRSMI-REL, Mr. Mullins	1
DRSMI-REL, Mr. Rast	1
DRSMI-REL, CAPT Schexnayder	1
DRSMI-RN, Mr. Race	1
DRSMI-RR, Dr. Hartman	1
DRSMI-RPR, RSIC (DTIC)	1
DRSMI-RPT, Record Set	11
Reference Copy	1
	1

☆U.S. GOVERNMENT PRINTING OFFICE: 1981—546-116/200

END

DATE
FILMED
3-82

DTIC